

Kinetic Interacting Particle Langevin Monte Carlo

Paul Felix Valsecchi Oliva and O. Deniz Akyildiz

Department of Mathematics, Imperial College London

[paul.valsecchi-oliva21](mailto:paul.valsecchi-oliva21@imperial.ac.uk), [deniz.akyildiz](mailto:deniz.akyildiz@imperial.ac.uk)@imperial.ac.uk

September 5, 2024

Abstract

This paper introduces and analyses interacting underdamped Langevin algorithms, termed Kinetic Interacting Particle Langevin Monte Carlo (KIPLMC) methods, for statistical inference in latent variable models. We propose a diffusion process that evolves jointly in the space of parameters and latent variables and exploit the fact that the stationary distribution of this diffusion concentrates around the maximum marginal likelihood estimate of the parameters. We then provide two explicit discretisations of this diffusion as practical algorithms to estimate parameters of statistical models. For each algorithm, we obtain nonasymptotic rates of convergence for the case where the joint log-likelihood is strongly concave with respect to latent variables and parameters. In particular, we provide convergence analysis for the diffusion together with the discretisation error, providing convergence rate estimates for the algorithms in Wasserstein-2 distance. We achieve accelerated convergence rates clearly demonstrating improvement in dimension dependence, similar to the underdamped samplers. To demonstrate the utility of the introduced methodology, we provide numerical experiments that demonstrate the effectiveness of the proposed diffusion for statistical inference and the stability of the numerical integrators utilised for discretisation. Our setting covers a broad number of applications, including unsupervised learning, statistical inference, and inverse problems.

1 Introduction

Parametric latent variable models (LVMs) are ubiquitous in many areas of statistical science, e.g., complex probabilistic models for text, audio, video and images [9, 65, 40] or inverse problems [66]. Intuitively, these models capture the underlying structure of the real data in terms of low-dimensional latent variables - a structure that often exists in real world [69]. However, latent variable models often require nontrivial procedures for maximum likelihood estimation as this quantity is often intractable [27]. Our main aim in this paper is to propose a set of accelerated and stable algorithms for the problem of maximum marginal likelihood estimation in the presence of latent variables and show convergence bounds for them by studying their nonasymptotic behaviour.

Let us consider a generic latent variable model as $p_\theta(x, y)$, parameterised by $\theta \in \mathbb{R}^{d_\theta}$, for fixed data $y \in \mathbb{R}^{d_y}$, and latent variables $x \in \mathbb{R}^{d_x}$. This model is considered for *fixed* observed data y , thus formally we see the statistical model as a real-valued mapping $p_\theta(x, y) : \mathbb{R}^{d_x} \times \mathbb{R}^{d_\theta} \rightarrow \mathbb{R}$. The task we are interested in is to estimate the parameter θ that explains the fixed dataset y . Often, this task is achieved via the maximum likelihood estimation (MLE). In accordance with this, in our setting, due to the presence of latent variables, we aim at finding the maximum *marginal* likelihood estimate, which termed as maximum marginal likelihood estimation (MMLE) problem [27]. More precisely, our problem takes the form

$$\bar{\theta}_* \in \operatorname{argmax}_{\theta \in \mathbb{R}^{d_\theta}} \log p_\theta(y), \quad (1)$$

where $p_\theta(y) := \int p_\theta(x, y) dx$ is the *marginal likelihood* (also called the model evidence in Bayesian statistics [7]). It is apparent from (1) that the problem cannot be solved via optimisation techniques alone, as the marginal likelihood contains an intractable integral for most statistical models.

Classically, this problem is solved with the iterative expectation maximisation (EM) algorithm [27], which provably converges to a local maximum. This algorithm consists of the E and M steps: (1) the E-step (optimally) produces an estimate for the posterior distribution of latent variables $p_\theta(x|y)$ and (2) the M-step maximises the expected log-likelihood estimate w.r.t. the parameter θ . More compactly, starting at θ_0 , the EM algorithm produces the estimates $(\theta_n)_{n \in \mathbb{N}}$, solving $\theta_{n+1} \in \operatorname{argmax}_{\theta \in \mathbb{R}^{d_\theta}} \mathbb{E}_{p_{\theta_n}(x|y)} [\log p_\theta(x, y)]$. It is easy to establish that $\log p_{\theta_{n+1}}(y) \geq \log p_{\theta_n}(y)$, hence the method converges to a local maximum. In this setting, two tasks need to be solved simultaneously: (i) inference, i.e., inferring the distribution of x given y for θ_n , in other words, the posterior distribution $p_{\theta_n}(x|y)$, (ii) estimation, i.e., estimating the maximiser θ_{n+1} , whose computation requires the inference step. Often, this recursion is impossible to realise, due to two main challenges, namely, the expectation (E) and maximisation (M) steps, which are intractable. These steps can be approximated with a variety of methods, which, due to the simplicity of this algorithm, have been extensively explored. For example, Monte-Carlo EM [68] and stochastic EM [15] have been widely studied, see, e.g., [16, 17, 64, 10, 13, 28].

In the most general case, the EM algorithm is implemented using Markov chain Monte Carlo (MCMC) techniques for the E-step, and numerical optimisation techniques for the M-step, e.g., [52, 50, 48]. With the popularity of unadjusted Langevin algorithm (ULA) in Bayesian statistics and machine learning [31, 33, 32, 22, 23, 25], variants of the implementation of expectation-maximisation algorithms using unadjusted chains to perform the E-step have also been proposed. Most notably, [26] studied an algorithm termed stochastic optimisation via unadjusted Langevin (SOUL), which performs unadjusted Langevin steps for the E-step and stochastic gradient ascent for the M-step, building on the ideas of [6]. This algorithm required to run a Markov chain for each E-step, resulting in a double-loop algorithm. The bias incurred by unadjusted chains complicates the theoretical analysis and requires a delicate balance of the step-sizes of the Langevin algorithm and gradient step to guarantee convergence [26].

An alternative approach was developed in [47], where instead of running Markov chains to perform E-step, the authors proposed to use an interacting particle system, consisting of N particles. Particle systems, such as the one proposed in [47], are often used to accelerate convergence for gradient-based methods or to replace these entirely ([11, 56, 46, 2, 39] for a review on their advantages and behaviour). In a similar vein, [47] shows that using an algorithm based on an interacting particle system (IPS), termed particle gradient descent (PGD), alleviates the need of running interleaving Markov chains, which can also lead to provable guarantees, see, e.g., [14]. Inspired by the approach in [47], a closely related interacting particle system was proposed in [3], where a properly scaled noise is injected in the θ -dimension. This seemingly small modification is significant, making the algorithm an instance of a Langevin diffusion (an observation we build on in this paper). The authors termed this method interacting particle Langevin algorithm (IPLA) and proved error bounds for the algorithm. In particular, they showed that the parameter-marginal of IPLA iterates, targets a measure of the form $\pi_\Theta \propto \exp(-N \log p_\theta(y))$, which concentrates around the MMLE estimate with a rate $\mathcal{O}(N^{-1/2})$ where N is the number of particles. The authors of [3] further provided the exponential convergence rate and the discretisation error under the within strongly convex setting. The IPLA methodology has been already utilised in other contexts, see, e.g., [45] for superlinear extensions and [35] for a set of proximal methods based on IPLA, and [4] for relations between IPLA and multiscale methods.

Finally, targeting this sort of measure to solve optimisation problems, is similar to simulated annealing techniques from optimisation (see [37, 42, 30, 43] for a discussion of these methods), which is a commonly proposed approach to MMLE. In particular, [30, 43] consider particle systems and observe sampling improvements in non-convex optimisation, motivating this alternative approach.

Contributions. In this paper, the overdamped Langevin diffusion proposed by [3] is modified by considering the underdamped setting - resulting in another stochastic differential equation (SDE) termed, kinetic interacting particle Langevin diffusion (KIPLD). In continuous time, our proposed diffusion corresponds to the noisy version of the system proposed in [49], and an acceleration of the overdamped diffusion introduced by [3], see, e.g., [51]. We then propose two underdamped Langevin samplers, which we term kinetic interacting

particle Langevin Monte Carlo (KIPLMC), based on this diffusion. Our contributions can be summarised as follows:

- We propose the **KIPLD**, a diffusion process to optimise the marginal likelihood in latent variable models. Our diffusion process corresponds to θ -noised version of the SDE proposed in [49]. However, in [49], the authors left the problem of nonasymptotic analysis open. In this paper, we provide a nonasymptotic analysis and show that the proposed modification enables us to prove that the stationary measure of this diffusion concentrates around the MMLE (Propositions 1 and 2) and the KIPLD converges to this measure exponentially fast (Proposition 3).
- We propose two discretisations of this diffusion to obtain practical algorithms, which we term KIPLMC methods. Our first algorithm **KIPLMC1** corresponds to an exponential integrator discretisation of our SDE. This algorithm is also similar to the momentum particle gradient descent (MPGD) algorithm provided by [49] which does not have noise in θ -dimension¹. However, we provide discretisation error bounds for our method showing convergence rates in both time and step-size (Theorem 1), closing the problem of nonasymptotic analysis of this method in the strongly convex case. In particular, we show that **KIPLMC1** attains accelerated rates of convergence compared to its overdamped counterparts IPLA [3] and PGD [47]. While these overdamped diffusion-based MMLE methods achieve an ε error in Wasserstein-2 distance in $\tilde{\mathcal{O}}(d_x \varepsilon^{-2})$ steps, we prove that **KIPLMC1** accelerates this process, reaching ε error in $\tilde{\mathcal{O}}(\sqrt{d_x} \varepsilon^{-1})$ steps, similar to the performance of underdamped Langevin-based sampling algorithms [20, 25].
- We then introduce a splitting-based explicit discretisation scheme within this setting, which leads to a nontrivial algorithm, which we term **KIPLMC2**. We provide a nonasymptotic analysis of this method (Theorem 2). We show that while MPGD algorithm provided by [49] only achieves stability with gradient correction steps, our **KIPLMC2** discretisation attains similar stability while having theoretical guarantees.
- Finally, we provide numerical results that show, in particular, the stability attained by KIPLMC2. We show in particular that this discretisation (which is based on [53]) is more stable than KIPLMC1 and MPGD of [49] when the latter is implemented as a standard discretisation of the diffusion provided in [49] without the use of the numerical trick called gradient correction. We show further that KIPLMC2 produces similar stable behaviour as the MPGD with gradient correction while also having solid theoretical guarantees.

The paper is structured as follows. In Section 2, we present the ULA, its underdamped counterpart, and interacting particle systems for the MMLE problem. Following this introduction, in Section 3, we present a new diffusion targeting the solution of the MMLE problem and present the associated algorithms KIPLMC1 and KIPLMC2. Section 4 presents the nonasymptotic analysis of KIPLMC methods, providing a clear evidence of improved theoretical bounds due to the acceleration. Finally, we provide solid empirical evidence in the experiments of Section 5, showing that KIPLMC methods constitute a set of accelerated and theoretically backed tools to solve challenging statistical inference problems.

Notation

Denote by $\mathcal{P}(\mathbb{R}^d)$, for $d \geq 1$, the space of all probability measures over $(\mathbb{R}^d, \mathcal{B}(\mathbb{R}^d))$, where $\mathcal{B}(\mathbb{R}^d)$ denotes the Borel σ -algebra over \mathbb{R}^d . Also consider the Euclidean inner-product space over \mathbb{R}^d , with inner product $\langle \cdot, \cdot \rangle$ and associated norm $\| \cdot \|$. We will be using this notation interchangeably over different dimensions d , assuming that the appropriate inner-product space is chosen. For notational convenience, denote $\{1, \dots, N\}$ as $[N]$ and the set of positive integers as \mathbb{N} .

¹While [49] uses a gradient correction mechanism to stabilise the discretisation of the SDE, we directly analyse the discretisation without any gradient correction steps.

Recall that, under a fixed dataset, our model is parameterised over $\theta \in \mathbb{R}^{d_\theta}$ and $x \in \mathbb{R}^{d_x}$. Let us consider an unnormalised probability model $U(\theta, x)$, where

$$U(\theta, x) = -\log p_\theta(x, y).$$

For any $p > 0$ define the Wasserstein- p metric as

$$W_p(\pi, \nu) = \inf_{\Gamma \in \mathbf{T}(\pi, \nu)} \left(\int \|x - y\|_p^p d\Gamma(x, y) \right)^{\frac{1}{p}},$$

where $\mathbf{T}(\pi, \nu)$ denotes the set of couplings over $\mathbb{R}^{d \times d}$, with marginals π and ν .

2 Technical Background

Before presenting our proposed diffusion and algorithms, we introduce some concepts that will be useful to us in this paper.

2.1 Unadjusted Langevin Algorithm

Consider the problem of simulating random variables with a law in $\mathcal{P}(\mathbb{R}^d)$ of the form

$$\pi(dz) \propto e^{-U(z)} dz, \tag{2}$$

where $U : \mathbb{R}^d \rightarrow \mathbb{R}$ is a potential function. This is a classical problem in computational statistics literature, with abundance of MCMC methods available, see, e.g., [58] for a book long treatment. In this paper, we focus on a particular class of MCMC algorithm, via the use of a discretisation of a particular SDE. The methods we are interested in rely on the fact that the following *Langevin* diffusion process

$$d\mathbf{Z}_t = -\nabla U(\mathbf{Z}_t) dt + \sqrt{2} d\mathbf{B}_t, \tag{3}$$

where $(\mathbf{B}_t)_{t \geq 0}$ is a standard Brownian motion, leaves the target measure (2) invariant. While this idea is well-known in MCMC literature and exploited for a long time as the proposal of the Metropolis adjusted Langevin algorithm (MALA) [60, 59, 70], recently several approaches simply drop the Metropolis step in this method and use the plain discretisation of the diffusion (3) as a sampling algorithm. This results in the following discretisation (termed unadjusted Langevin algorithm (ULA) [32, 31] or Langevin Monte Carlo (LMC) [22])

$$Z_{n+1}^\eta = Z_n^\eta - \eta \nabla U(Z_n^\eta) + \sqrt{2\eta} W_{n+1},$$

where $(W_n)_{n \in \mathbb{N}}$ are standard d -dimensional Normal random variables and $\eta > 0$ corresponds to the step-size of the algorithm.

The performance and complexity of sampling with ULA, for convex and strongly convex U , have been extensively studied [31, 25]. The ULA has proved to be an efficient way to sample from these distributions, alleviating numerical and computational issues of the accept-reject steps. This improved computational performance comes at the expense of incurring a bias of order $\eta^{1/2}$ in the stationary measure of the algorithm [32]. Despite this, the ULA is a natural choice for sampling, as it can be implemented through a variety of discretisations and has, as discussed, favourable theoretical properties, see, e.g., [31, 67, 33, 12, 21, 60, 59] and [24], for convergence results under different assumptions on U .

2.2 Kinetic Langevin Monte Carlo

An alternative to the Langevin diffusions given in (3), which are generally termed *overdamped* Langevin diffusions, is another class of Langevin diffusions called *underdamped* diffusions [55]. This class of diffusions is

akin to second-order differential equations and defined over position and momentum variables. The momentum dynamics are given by Newton’s Law for the motion of a particle, subject to friction and a stochastic forcing, acting as the gradient of the position particle [20]. In particular, for a d -dimensional target measure, the underdamped Langevin diffusion is defined to evolve on $\mathbb{R}^d \times \mathbb{R}^d$ given by the SDE

$$\begin{aligned} d\mathbf{Z}_t &= \mathbf{V}_t dt \\ d\mathbf{V}_t &= -\gamma \mathbf{V}_t dt - \nabla_z U(\mathbf{Z}_t) dt + \sqrt{2\gamma} d\mathbf{B}_t, \end{aligned} \tag{4}$$

where $\gamma > 0$ is called the friction coefficient and $(\mathbf{B}_t)_{t \geq 0}$ is a Brownian motion. From this equation, one can recover the *overdamped* dynamics in (3) by letting $\gamma \rightarrow \infty$ and considering the behaviour of the z -marginal [54, pg. 58]. Under certain regularity conditions [55], this system is known to be invariant w.r.t. an extended stationary measure of the form

$$\bar{\pi}(dz, dv) \propto \exp\left(-U(z) - \frac{1}{2}\|v\|^2\right) dz dv. \tag{5}$$

This means that we can recover the samples from our target measure (2) by sampling from (5) where the z -marginal of $\bar{\pi}$ is the target measure we would like to sample from.

Discretisation of (4) provides a set of algorithms termed as kinetic Langevin Monte Carlo (KLMC) [25]. These methods define discretisation methods tailored to the structure of the SDE given in (4), although Euler-Maruyama methods for this class of SDEs are also analysed [1, 38, 18]. As the update rules of the resulting algorithm are determined by a numerical approximation of a continuous-time process, how this algorithm performs is dependent on the smoothness of the sample paths and the mixing rate of the system. It is quite easy to see that the sample paths in the underdamped case are smoother, having an Hölder continuity of order $1 + \alpha$, for $\alpha \in [0, 1/2)$ (see introduction of [25]). Furthermore, similar to the ULA algorithm, this system also has exponentially fast convergence to the stationary measure [25]. By using an underdamped, second-order system, [20] exploit these properties to accelerate the first-order process, connecting this work to Nesterov acceleration and the growing body of literature dedicated to it. Indeed, [20] show that for certain choices of γ the underdamped system converges faster to the stationary measure than the overdamped system and identify the regimes in which the underdamped algorithm outperforms the overdamped for their sampling schemes. This acceleration has not only been noted in W_2 , by [25, 19] and others, but also in Kullback-Leibler (KL) divergence by [51]. The underdamped process leads to some interesting properties, such as an “induced regularisation” via damping effects, as well as, convergence with better dependence on dimension and step-size, as shown in [19]. Hence, the underdamped Langevin diffusion, presents a worthwhile starting point for sampling algorithms and represents a competitive alternative to the popular ULA.

2.3 MMLE via Interacting Particle Langevin Algorithm

These sampling algorithms, however, are not sufficient for parameter estimation. While sampling algorithms above provide an efficient way to sample from a given probability measure, they need to be supplemented by optimisation techniques when the target probability measure is indexed by a parameter θ . As mentioned in the introduction, our main aim in this paper is to develop algorithms to solve the maximum marginal likelihood estimation problem MMLE which is given by

$$\bar{\theta}_* \in \operatorname{argmax}_{\theta \in \mathbb{R}^{d_\theta}} \log p_\theta(y),$$

for fixed $y \in \mathbb{R}^{d_y}$ and $p_\theta(y) = \int p_\theta(x, y) dx$. Therefore the MMLE problem involves the maximisation of an often intractable integral. Let $U(\theta, x) = -\log p_\theta(x, y)$ and note that the (intractable) θ -gradient of $\log p_\theta(y)$ can be written as

$$\nabla_\theta \log p_\theta(y) = \frac{-\int_{\mathbb{R}^{d_x}} \nabla_\theta U(\theta, x) p_\theta(x, y) dx}{p_\theta(y)} = -\int_{\mathbb{R}^{d_x}} \nabla_\theta U(\theta, x) p_\theta(x|y) dx, \tag{6}$$

which is easy to prove (see, e.g., [29, Proposition D.4] and [3, Remark 1]). The expression in (6) is the motivation behind approximate schemes for EM, where one can first sample from $p_\theta(x|y)$ for fixed θ with an MCMC chain and then compute the gradient in (6) with these samples [26, 6]. However, these approaches require non-trivial assumptions on the step-size, as well as having a sample size that may need to grow to ensure that the gradient approximation does not incur asymptotic bias.

In contrast to this approach, [47] propose an IPS, the particle gradient descent (PGD) algorithm, to approximate the gradient of the θ -dynamics by running independent particles to integrate out latent variables. Inspired by this, [3] attempt to solve the MMLE problem with a similar IPS, termed the interacting particle Langevin Algorithm (IPLA), which is a modification of PGD where θ -dynamics contain a carefully scaled noise. This approach produces a system that is akin to the ULA and makes the theoretical analysis streamlined using the analysis produced for ULA, see, e.g., [31, 23, 32]. The proposed algorithm is a discretisation of a system of interacting Langevin SDEs which evolves in $\mathbb{R}^{d_\theta} \times \mathbb{R}^{Nd_x}$ where N distinct particles are retained for latent variables. More precisely, IPLA recursions are based on the SDE:

$$d\boldsymbol{\theta}_t = -\frac{1}{N} \sum_{i=1}^N \nabla_\theta U(\boldsymbol{\theta}_t, \mathbf{X}_t^i) dt + \sqrt{\frac{2}{N}} d\mathbf{B}_t^0, \quad (7)$$

$$d\mathbf{X}_t^i = -\nabla_x U(\boldsymbol{\theta}_t, \mathbf{X}_t^i) dt + \sqrt{2} d\mathbf{B}_t^i, \quad \text{for } i \in [N]. \quad (8)$$

where $(\mathbf{B}_t^0)_{t \geq 0}$ is a Brownian motion evolving on \mathbb{R}^{d_θ} and $(\mathbf{B}_t^i)_{t \geq 0}$ for $i \in [N]$ are Brownian motions evolving on \mathbb{R}^{d_x} . Intuitively, it can be seen that the drift term for the θ -dynamics can be interpreted as the empirical approximation of the “true” drift (6) with N particles drawn from a measure drifting towards $p_\theta(x|y)$. In this case, [3] observe that the stationary measure of this system is given as

$$\pi^N(d\theta, dx_1, \dots, dx_N) \propto \exp\left(-\sum_{i=1}^N U(\theta, x_i)\right) d\theta dx_1 \dots dx_N.$$

It is easy to show that, the θ -marginal of this measure concentrates on the MMLE $\bar{\theta}_*$ as N grows, similar to annealing techniques developed in traditional optimisation [41]. The authors of [3] identify the convergence rate to the joint stationary measure, as well as, an error bound for the discretisation error, from which an error can be determined between the θ -iterate of the algorithm and the MMLE. With this nonasymptotic analysis, [3] identify parameters needed to implement the algorithm and introduce an order of convergence guarantee in W_2 . The algorithm is empirically shown to be competitive with similar methods, such as SOUL [26] and the PGD proposed in [47], while also amenable to a streamlined theoretical analysis akin to ULA. Furthermore, the similarity between IPLA and ULA lays the foundation for several avenues of further exploration, such as considering a kinetic Langevin algorithm and exploring other numerical discretizations of the proposed SDEs, as we aim to do in this paper.

3 Kinetic Interacting Particle Langevin Monte Carlo

Our goal is to combine the advantages of underdamped Langevin diffusions with the interacting particle systems proposed by [3, 47, 49], to estimate the MMLE $\bar{\theta}_*$. In this section we present a diffusion and two algorithms to this end. Indeed, this diffusion will be an underdamped version of the system of overdamped Langevin diffusions of the IPLA SDEs given in (7)–(8).

3.1 Kinetic Interacting Particle Langevin Diffusion

We introduce the KIPLD system, the underdamped counterpart of the IPLA diffusion given. More precisely, the KIPLD diffusion evolves on $\mathbb{R}^{2d_\theta} \times \mathbb{R}^{2Nd_x}$ and given by

$$\begin{aligned} d\boldsymbol{\theta}_t &= \mathbf{V}_t^\theta dt \\ d\mathbf{X}_t^i &= \mathbf{V}_t^{x_i} dt, \\ d\mathbf{V}_t^\theta &= -\gamma \mathbf{V}_t^\theta dt - \frac{1}{N} \sum_{i=1}^N \nabla_{\theta} U(\boldsymbol{\theta}_t, \mathbf{X}_t^i) dt + \sqrt{\frac{2\gamma}{N}} d\mathbf{B}_t^0 \\ d\mathbf{V}_t^{x_i} &= -\gamma \mathbf{V}_t^{x_i} dt - \nabla_x U(\boldsymbol{\theta}_t, \mathbf{X}_t^i) dt + \sqrt{2\gamma} d\mathbf{B}_t^i, \quad \text{for } i \in [N] \end{aligned} \tag{KIPLD}$$

where $(\mathbf{B}_t^i)_{t \geq 0}$ for $i \in [N]$ is a family of \mathbb{R}^{d_x} -valued Brownian motions and $(\mathbf{B}_t^0)_{t \geq 0}$ is an \mathbb{R}^{d_θ} -valued Brownian motion. For notational convenience we will say that the particles and momenta have combined dimension of $d_z = d_\theta + Nd_x$ each. Similarly to the algorithm proposed by [3], we have a system of N particles for the empirical approximation of latent variable distribution. This system corresponds to relaxing the limit on γ , the ‘‘friction’’ parameter, for the algorithm proposed by [3]. Adding the friction hyper-parameter γ should allow for improved regularisation and dampening momentum effects, as discussed in [51]. We will note some of this behaviour in the experimental section, where the momentum effect can be observed and tuned to produce optimal convergence behaviour.

An alternative perspective is that, in line with the work done by [3], we consider here a noisy analogue of a simplified version of the MPGD SDE, see, Eq. (21) in [49] (we take $\eta_\theta = \eta_x = 1^2$ and $\gamma_x = \gamma_\theta = \gamma$). In particular, we are injecting the θ -dynamics with the appropriately scaled Brownian motion, i.e., $\sqrt{2\gamma/N} d\mathbf{B}_t^0$. The advantage of studying and implementing this version is due to the fact that the new system can be shown to be an example of a standard underdamped Langevin diffusion, which enables us to use the numerous results available for Langevin diffusions of kinetic-type and associated discretisations for this class of diffusions. We also recover the algorithm proposed by [49] by considering this version as a noised version of the MPGD (indeed for large N , this difference should be more attenuated). While our version is a simplified version of the SDE given in [49], the results presented here should naturally extend to the more general case.

3.2 Kinetic Interacting Particle Langevin Monte Carlo Methods

We now introduce two numerical integrators for the KIPLD: firstly, we consider an Exponential Integrator, as discussed in [25]; secondly, a splitting scheme is applied, as described in [53]. These algorithms for kinetic Langevin samplers have two parameters, namely, the step-size $\eta > 0$, which assumed to be small, and the friction coefficient $\gamma > 0$, determining momentum effects.

3.2.1 Exponential Integrator (KIPLMC1)

In this section, we consider a discretisation similar to the one employed by [20], which is an exponential integrator tailored to the kinetic Langevin diffusion. This discretisation is a variant of the Hamiltonian Monte Carlo which has improved convergence properties when compared to the Langevin MCMC proposed by [32]. Specifically, while the standard overdamped Langevin methods (e.g. ULA) requires $\tilde{\mathcal{O}}(d/\varepsilon^2)$ number of steps³ to attain ε error in Wasserstein-2 distance, it is shown in [20, Theorem 1] that the underdamped Langevin MCMC using the exponential integrator requires $\tilde{\mathcal{O}}(\sqrt{d}/\varepsilon)$ steps to attain the same error rate. This method is proposed for sampling from underdamped Langevin diffusions, as, unlike Euler-Maruyama, this approach is able to exploit the higher order of convergence of the underlying process [25]. The bounds on the convergence rate for this algorithm are further improved in [25] with a tightened the bound with respect to the condition number L/μ and improve sensitivity to the initial choice.

²Note that this is not the step-size in their context as in our notation.

³The notation $\tilde{\mathcal{O}}$ suppresses the logarithmic dependence to d and ε .

Algorithm 1 KIPLMC1 Algorithm

Require: $\gamma, \eta > 0, N, K \in \mathbb{N}$

- 1: Draw $\theta_0, X_0^i, V_0^\theta, V_0^{x_i}$, for $i \in [N]$
 - 2: **for** $n = 0 : K - 1$ **do**
 - 3: Draw $\varepsilon_n, \varepsilon'_n$ from $d_\theta + Nd_x$ -dimensional Gaussians with covariance C given in (9)
 - 4: $\theta_{n+1} = \theta_n + \psi_1(\eta)V_n^\theta - \frac{\psi_2(\eta)}{N} \sum_{i=1}^N \nabla_\theta U(\theta_n, X_n^i) + \sqrt{\frac{2\gamma}{N}}\varepsilon_n^{0,\prime}$
 - 5: $X_{n+1}^i = X_n^i + \psi_1(\eta)V_n^{x_i} - \psi_2(\eta)\nabla_x U(\theta_n, X_n^i) + \sqrt{2\gamma}\varepsilon_n^{i,\prime}$
 - 6: $V_{n+1}^\theta = \psi_0(\eta)V_n^\theta - \frac{\psi_1(\eta)}{N} \sum_{i=1}^N \nabla_\theta U(\theta_n, X_n^i) + \sqrt{\frac{2\gamma}{N}}\varepsilon_n^0$
 - 7: $V_{n+1}^{x_i} = \psi_0(\eta)V_n^{x_i} - \psi_1(\eta)\nabla_x U(\theta_n, X_n^i) + \sqrt{2\gamma}\varepsilon_n^i$
 - 8: **for** $i \in [N]$
 - return** θ_K
-

Motivated by this we aim at applying this scheme to the diffusion [KIPLD](#) and seek to recover improved results (see Section 4.4 for details). Following [25], we begin by defining functions

$$\begin{aligned}\psi_0(t) &= e^{-\gamma t} \\ \psi_1(t) &= \int_0^t e^{-\gamma s} ds = \frac{1}{\gamma}(e^{-\gamma t} - 1) \\ \psi_2(t) &= \frac{1}{\gamma} \int_0^t (e^{-\gamma s} - 1) ds = \frac{1}{\gamma^2}(e^{-\gamma t} - 1) - \frac{t}{\gamma}.\end{aligned}$$

These terms emerge from the Itô formula used to estimate the expectations and their covariances (see [20, Lemma 11] for a full derivation). The pairs $\varepsilon_n^i, \varepsilon_n^{i,\prime}$, for $i \in [N]$, are i.i.d. standard normal Gaussians with pair-wise covariance matrix

$$C = \int_0^\eta \begin{pmatrix} \psi_0(t)^2 & \psi_0(t)\psi_1(t) \\ \psi_0(t)\psi_1(t) & \psi_1(t)^2 \end{pmatrix} dt. \quad (9)$$

This covariance matrix is the covariance between the dynamics of the position particle and the momentum particle, as shown in [20, Lemma 11]. The scheme is recovered by updating the particle positions with the expectations of the particles conditioned on the previous time-step and adding Gaussian noise with covariance C . Thus, the scheme produces the same first and second momenta as the diffusion we seek to target. Formally, we define the KIPLMC1 scheme as

$$\begin{aligned}\theta_{n+1} &= \theta_n + \psi_1(\eta)V_n^\theta - \frac{\psi_2(\eta)}{N} \sum_{i=1}^N \nabla_\theta U(\theta_n, X_n^i) + \sqrt{\frac{2\gamma}{N}}\varepsilon_n^{0,\prime} \\ X_{n+1}^i &= X_n^i + \psi_1(\eta)V_n^{x_i} - \psi_2(\eta)\nabla_x U(\theta_n, X_n^i) + \sqrt{2\gamma}\varepsilon_n^{i,\prime} \\ V_{n+1}^\theta &= \psi_0(\eta)V_n^\theta - \frac{\psi_1(\eta)}{N} \sum_{i=1}^N \nabla_\theta U(\theta_n, X_n^i) + \sqrt{\frac{2\gamma}{N}}\varepsilon_n^0 \\ V_{n+1}^{x_i} &= \psi_0(\eta)V_n^{x_i} - \psi_1(\eta)\nabla_x U(\theta_n, X_n^i) + \sqrt{2\gamma}\varepsilon_n^i\end{aligned} \quad (\text{KIPLMC1})$$

for $i \in [N]$, where ε_n and ε'_n are standard Gaussians with pairwise covariance given by C . The scheme converges for certain choices of η , depending on the assumptions set on U . The full algorithm is given in Algorithm 1.

3.2.2 A Splitting Scheme (KIPLMC2)

The KIPLMC splitting algorithm (KIPLMC2) is an adaptation of the underdamped Langevin sampler introduced by [53], based on classic splitting techniques from MCMC. As with the exponential integrator

Algorithm 2 KIPLMC2 Algorithm

Require: $\gamma, \eta > 0, N, K \in \mathbb{N}$

- 1: Draw $\theta_0, X_0^i, V_0^\theta, V_0^{x_i}$, for $i \in [N]$
 - 2: **for** $n = 0 : K - 1$ **do**
 - 3: Draw $\varepsilon_n, \varepsilon'_n$ from $d_\theta + Nd_x$ -dimensional Gaussians
 - 4: (O+B):
 - 5: $V_{n+\frac{1}{2}}^\theta = \delta V_n^\theta + \frac{1}{\sqrt{N}} \sqrt{1 - \delta^2} \varepsilon_n^0 - \frac{\eta}{2N} \sum_{i=1}^N \nabla_\theta U(\theta_n, X_n^i)$
 - 6: $V_{n+\frac{1}{2}}^{x_i} = \delta V_n^{x_i} + \sqrt{1 - \delta^2} \varepsilon_n^i - \eta \nabla_{x_i} U(\theta_n, X_n^i)$
 - 7: (A):
 - 8: $\theta_{n+1} = \theta_n + \eta V_{n+\frac{1}{2}}^\theta$
 - 9: $X_{n+1}^i = X_n^i + \eta V_{n+\frac{1}{2}}^{x_i}$
 - 10: (B+O):
 - 11: $V_{n+1}^\theta = \delta(V_{n+\frac{1}{2}}^\theta - \frac{\eta}{2N} \sum_{i=1}^N \nabla_\theta U(\theta_{n+1}, X_{n+1}^i)) + \frac{1}{\sqrt{N}} \sqrt{1 - \delta^2} \varepsilon_n^{0,\prime}$
 - 12: $V_{n+1}^{x_i} = \delta(V_{n+\frac{1}{2}}^{x_i} - \frac{\eta^2}{2} \nabla_{x_i} U(\theta_{n+1}, X_{n+1}^i)) + \frac{1}{\sqrt{N}} \sqrt{1 - \delta^2} \varepsilon_n^{i,\prime}$
- return** θ_K
-

scheme proposed by [25], the scheme proposed by [53] achieves ε error in Wasserstein-2 distance using ε in $\tilde{\mathcal{O}}(\sqrt{d}/\varepsilon)$ steps, see, e.g., [53, Table 2]. Specifically, [53] propose an OBABO scheme as the discretisation scheme, which is a second order scheme only requiring the computation of first order derivatives of U . The idea is to split the numerical scheme into individually tractable components. In our underdamped case (KIPLD), we have: (A) the update of θ and X^i with known V^θ and V^{x_i} ; (B) update V^θ and V^{x_i} with the first order Taylor scheme for the integrals of $\frac{1}{N} \sum_{i=1}^N \nabla_\theta U(\theta, X^i)$ and $\nabla_{x_i} U(\theta, X^i)$; (O) solve the Ornstein-Uhlenbeck equation with the terms V^θ and V^{x_i} . Thus, the algorithm “splits” the equation into components with known solutions. The order in which these steps are taken is critical and in our case we will limit ourselves to considering the OBABO scheme from [53].

In our case we introduce the KIPLMC2 algorithm based on the OBABO scheme, given as

$$\begin{aligned}
 \theta_{n+1} &= \theta_n + \eta(\delta V_n^\theta + \frac{1}{\sqrt{N}} \sqrt{1 - \delta^2} \varepsilon_n^0) - \frac{\eta^2}{2N} \sum_{i=1}^N \nabla_\theta U(\theta_n, X_n^i) \\
 X_{n+1}^i &= X_n^i + \eta(\delta V_n^{x_i} + \sqrt{1 - \delta^2} \varepsilon_n^i) - \frac{\eta^2}{2} \nabla_{x_i} U(\theta_n, X_n^i) \tag{KIPLMC2} \\
 V_{n+1}^\theta &= \delta^2 V_n^\theta - \frac{\delta \eta}{2} \left(\frac{1}{N} \sum_{i=1}^N \nabla_\theta U(\theta_n, X_n^i) + \frac{1}{N} \sum_{i=1}^N \nabla U(\theta_{n+1}, X_{n+1}^i) \right) + \frac{1}{\sqrt{N}} \sqrt{1 - \delta^2} (\delta \varepsilon_n^0 - \varepsilon_n^{0,\prime}) \\
 V_{n+1}^{x_i} &= \delta^2 V_n^{x_i} - \frac{\delta \eta}{2} (\nabla_{x_i} U(\theta_n, X_n^i) + \nabla_{x_i} U(\theta_{n+1}, X_{n+1}^i)) + \sqrt{1 - \delta^2} (\delta \varepsilon_n^i + \varepsilon_n^{i,\prime})
 \end{aligned}$$

for $i \in [N]$, where $\delta = e^{-\eta\gamma/2}$ and in this case ε_n^i and $\varepsilon_n^{i,\prime}$ are i.i.d. standard Gaussians for $i \in [N]$ in this case. The full algorithm is given in Algorithm 2, where we can see the OBABO decomposition more clearly. To produce a half-update of V^θ and V^{x_i} the (O) and (B) steps are computed. These are then used to update the parameter and particle estimates (A), followed by the (B) and (O) steps performed in reverse order to update the momenta estimates. Giving us the desirable property of being a second-order, explicit scheme, which does not require computation of $\nabla^2 U$.

4 Nonasymptotic Analysis

In this section, we provide the convergence results for both the analytic and numerical schemes in the nonasymptotic regime. In Section 4.1, we lay out our assumptions about our target measure. In Section 4.2,

we introduce the proof strategy for reader’s convenience, which can be also useful for extending and proving similar results leveraging the same structure as we do. In Section 4.3, we provide the full nonasymptotic bounds – in particular, in Section 4.3.1, we identify the stationary measure for **KIPLD** and show an exponential convergence rate to it, as well as, its concentration onto the MMLE solution $\bar{\theta}_*$ as N grows. Following this, in Section 4.3.2, the error bounds for the two algorithms are provided, thus allowing us to identify the convergence rate of **KIPLMC1** and **KIPLMC2** to the MMLE solution $\bar{\theta}_*$, which is discussed in 4.4.

4.1 Assumptions

We first lay out our assumptions to prove the convergence of the numerical schemes outlined in 3. Our assumptions are generic for the analysis of Langevin diffusions, i.e., we assume strong convexity and L -Lipschitz gradients for the potential U . These assumptions are akin to the assumptions made in [31, 23, 24] for proving the convergence of ULA. As such, the assumptions are necessary for basic building blocks of the theory – but it is possible to relax them, as can be seen in [71, 1].

We remark nonetheless that, while in the works cited above, assumptions correspond to strong log-concavity (and Lipschitz regularity) of the target measure (i.e. strongly convex U implies that the target measure is assumed to be strongly log-concave), in our setting this corresponds to imposing a strong structure on the joint statistical model $p_\theta(x, y)$ in θ and x . Note that, in our case the potential is given by $U(\theta, x) = -\log p_\theta(x, y)$, in other words, our potential is not merely the log-target, it is the joint negative log-likelihood. Thus, the assumptions below require statisticians to check whether their models satisfy these assumptions. We check in the experimental section that for some generic models such as Bayesian logistic regression, this is possible. As noted above, however, these strong assumptions on the statistical model should not be difficult to relax using the standard non-log-concave sampling results – but this direction is out of scope of the present work which considers the strongly convex case.

We start with the following assumption on the potential U .

H1. Let $z, z' \in \mathbb{R}^{d_\theta+d_x}$, we suppose that there exists a μ s.t.

$$\langle z - z', \nabla U(z) - \nabla U(z') \rangle \geq \mu \|z - z'\|^2.$$

This assumption also implies that $\nabla^2 U$ is positive definite, i.e., $\nabla^2 U(z) \succeq \mu I$ for all $z \in \mathbb{R}^{d_\theta+d_x}$.

This assumption is equivalent to an assumption of joint strong convexity in θ and x for U , which ensures exponentially fast convergence of the **KIPLD** to the global minimiser and places a quadratic lower growth bound on U . This assumption also means that we can apply the Leibniz differentiation rule under integration for the marginal of the probability model $p_\theta(x, y) = e^{-U(\theta, x)}$ [8, Theorem 16.8]. On a more statistical note, this assumption requires that the log-likelihood function $\log p_\theta(x, y)$ should be strongly concave in both the latent variable x and the parameter θ .

Next, we provide the regularity assumption on U .

H2. We suppose $U \in \mathcal{C}^1$ and for any $z, z' \in \mathbb{R}^{d_\theta+d_x}$ there exists a constant $L > 0$ s.t.

$$\|\nabla U(z) - \nabla U(z')\| \leq L \|z - z'\|.$$

This assumption is a common assumption in the analysis of stochastic differential equations, as it ensures stability of the diffusion **KIPLD**, leading to strong solutions, and stable numerical discretisations (see e.g. [55]). Note also that from the perspective of the probabilistic model, this assumption is the same as assuming that $\log p_\theta(x, y)$ is gradient Lipschitz. Note that, it is possible to also relax these assumptions, incorporating superlinearly growing gradients, see, e.g., [45].

4.2 The proof strategy

Given the assumptions above, we aim at bounding the *optimisation error* of the numerical schemes, i.e., the difference between the law of the numerical scheme and the optimal MMLE solution $\bar{\theta}_*$. Let $(\theta_n)_{n \geq 0}$ be the

sequence of iterates generated by a numerical scheme, for example, [KIPLMC1](#) or [KIPLMC2](#). Finally, let π_Θ denote the θ -marginal of the stationary measure of the diffusion [KIPLD](#), and $\delta_{\bar{\theta}_*}$ denote the Dirac measure at $\bar{\theta}_*$. We denote the law of θ_n by $\mathcal{L}(\theta_n)$. The optimisation error is then defined as $\mathbb{E}[\|\theta_n - \bar{\theta}_*\|^2]^{1/2}$.

In order to proceed, we first note that $\mathbb{E}[\|\theta_n - \bar{\theta}_*\|^2]^{1/2} = W_2(\mathcal{L}(\theta_n), \delta_{\bar{\theta}_*})$, where $\mathcal{L}(\theta_n)$ denotes the law of θ_n . This is due to the fact that the set of couplings between a measure ν and another measure δ_y contains a single element $\delta_y \otimes \nu$ [[61](#), Section 1.4], thus the infimum in Wasserstein-2 distance is attained by the coupling $\delta_{\bar{\theta}_*} \otimes \mathcal{L}(\theta_n)$. Using this, we can then write

$$\begin{aligned} \mathbb{E}[\|\theta_n - \bar{\theta}_*\|^2]^{1/2} &= W_2(\mathcal{L}(\theta_n), \delta_{\bar{\theta}_*}) \\ &\leq \underbrace{W_2(\pi_\Theta, \delta_{\bar{\theta}_*})}_{\text{concentration}} + \underbrace{W_2(\mathcal{L}(\theta_n), \pi_\Theta)}_{\text{convergence}}, \end{aligned} \tag{10}$$

using the triangle inequality as the Wasserstein distance is a metric. The first term in the right-hand side of [\(10\)](#) is the concentration of the stationary measure π_Θ onto the MMLE solution $\bar{\theta}_*$, which is given by [Proposition 2](#) below. The second term is the convergence of the numerical scheme to the stationary measure π_Θ which will be proved for each scheme separately.

4.3 Nonasymptotic convergence bounds

As outlined above in [\(10\)](#), we will first show the concentration of the stationary measure π_Θ onto the MMLE solution $\bar{\theta}_*$. We then show the convergence of the numerical schemes to the stationary measure π_Θ . Finally, we will provide the error bounds for the numerical schemes.

4.3.1 Concentration of the stationary measure

We are interested in the behaviour of the stationary measure of [KIPLD](#). This is a non-standard underdamped Langevin diffusion, thus, we need to first identify the stationary measure of the system. Recall that we are only interested in θ -marginal of this stationary measure and we denote it by π_Θ . We first have the following proposition.

Proposition 1. *Let π_Θ be the θ -marginal of the stationary measure of the [KIPLD](#). Then, we can write its density as*

$$\pi_\Theta(\theta) \propto \exp(-N\kappa(\theta)). \tag{11}$$

where $\kappa(\theta) = -\log p_\theta(y)$.

Proof. See [Appendix B.1](#). \square

This result shows that the [KIPLD](#) targets the right object: As N grows, π_Θ will concentrate on the minimisers of $\kappa(\theta)$ by a classical result [[41](#)]. This shows that the number of particles N acts as an inverse temperature parameter in the underdamped diffusion. Since the minimiser of $\kappa(\theta)$ is the maximiser of $\log p_\theta(y)$, we can see that the stationary measure of the [KIPLD](#) is concentrating on the MMLE solution $\bar{\theta}_*$. In particular, under the assumption [H1](#), we have the following nonasymptotic concentration result.

Proposition 2. *Under [H1](#), the function $\theta \mapsto p_\theta(y)$ is μ -strongly log concave. Furthermore, we have*

$$W_2(\pi_\Theta, \delta_{\bar{\theta}_*}) \leq \sqrt{\frac{2d_\theta}{\mu N}},$$

where $\bar{\theta}_* = \operatorname{argmax}_{\theta \in \Theta} \log p_\theta(y)$, which is unique.

Proof. See [Appendix B.2](#). \square

This shows that there is an explicit rate of convergence of the θ -marginal of the stationary measure of [KIPLD](#) to the MMLE solution $\bar{\theta}_*$. This is a key result, as it shows that the stationary measure of the system is concentrating on the MMLE solution as N grows. We note that such results are also potentially possible under nonconvex settings [[71](#), [1](#)].

4.3.2 Convergence of the KIPLD to the stationary measure

We next demonstrate that the KIPLD converges to its stationary measure π_Θ exponentially fast in the strongly log-concave case. Indeed, knowing that the system KIPLD is ergodic, we would like to quantify the rate at which this mixing occurs, specifically at what rate the W_2 distance of the process and its stationary distribution converges for a possibly large range of γ .

Proposition 3. *Let $(\theta_t)_{t \geq 0}$ be the θ -marginal of a solution to the KIPLD, initialised at $\mathbf{Z}_0 \sim \nu \otimes \mathcal{N}(0, \mathbb{I}_{d_z})$. Then under H1 and H2 and for $\gamma \geq \sqrt{\mu + L}$, we have*

$$W_2(\mathcal{L}(\theta_t), \pi_\Theta) \leq \sqrt{2} \exp\left(-\frac{\mu}{\gamma} t\right) \mathbb{E}[\|\mathbf{Z}_0 - \bar{Z}_*\|^2]^{1/2},$$

where $\bar{Z}_* \sim \bar{\pi}$ is the extended target measure described in Lemma A.3.

Proof. See Appendix B.3. \square

This proposition shows that, under the conditions expressed in Proposition 3, the KIPLD SDE converges exponentially fast to the target measure, which concentrates on the minimum as outlined in Proposition 2.

4.3.3 Nonasymptotic analysis of KIPLMC1

In this section we present our first main result showing the convergence rate of KIPLMC1. The result is provided in the following theorem.

Theorem 1. *Let $(\theta_n)_{n \in \mathbb{N}}$ be the iterates of KIPLMC1 and suppose that the process is initialised as $(Z_0, V_0^z)^T \sim \nu \otimes \mathcal{N}(0, \mathbb{I}_{d_z})$, where $\nu \in \mathcal{P}(\mathbb{R}^{d_z})$ has bounded second moments. Under Assumptions H1 and H2 and with $\gamma \geq \sqrt{\mu + L}$ and $\eta \leq \mu/(4\gamma L)$, we have*

$$\mathbb{E}[\|\theta_n - \bar{\theta}_*\|^2]^{1/2} \leq \sqrt{2} \left(1 - \frac{3\mu\eta}{4\gamma}\right)^n \mathbb{E}[\|Z_0 - \bar{Z}_*\|^2]^{1/2} + \sqrt{2} \frac{L\eta}{\mu} \sqrt{\frac{d_\theta + Nd_x}{N}} + \sqrt{\frac{2d_\theta}{\mu N}},$$

where $Z_0 = (\theta_0, N^{-1/2}X_0^1, \dots, N^{-1/2}X_0^N)^\top$, the initialisation step of the KIPLMC1 where $\bar{Z}_* \sim \bar{\pi}$ and $\bar{\pi}$ is the extended target measure described in Lemma A.3.

Proof. See Appendix B.4. \square

The result follows from the fact that the target measure π_Θ of our system concentrates on the maximiser which is given by Proposition 2 and using the results in [25] for kinetic Langevin diffusions and the exponential integrator discretisation. Further, we replicate the choice made in [25] of initialising the momentum particle according to $\mathcal{N}(0, \mathbb{I}_{d_z})$, the stationary measure under the momentum marginal.

4.3.4 Nonasymptotic analysis of KIPLMC2

In the following section, we present our second main result, showing the convergence rate of KIPLMC2. The rate is explicitly given in the subsequent theorem.

Theorem 2. *Let $(\theta_n)_{n \in \mathbb{N}}$ be the iterates of KIPLMC2 and suppose that the process is initialised as $(Z_0, V_0^z)^T \sim \nu \otimes \mathcal{N}(0, \mathbb{I}_{d_z})$, where $\nu \in \mathcal{P}(\mathbb{R}^{d_z})$ has bounded second moments. Under Assumptions H1 and H2 and with $\gamma \geq 2\sqrt{L}$ and $\eta \leq \frac{\mu}{33\gamma^3}$, we have*

$$\mathbb{E}[\|\theta_n - \bar{\theta}_*\|^2]^{1/2} \leq C \left(\left(1 - \frac{\eta\mu}{3\gamma}\right)^{\frac{n}{2}} \mathbb{E}[\|Z_0 - \bar{Z}_*\|^2]^{1/2} + \eta \sqrt{2(Nd_x + d_\theta)} \frac{6\gamma K}{\mu} \right) + \sqrt{\frac{2d_\theta}{\mu N}},$$

where $Z_0 = (\theta_0, N^{-1/2}X_0^1, \dots, N^{-1/2}X_0^N)^\top$, the initialisation step of the [KIPLMC2](#), $\bar{Z}_* \sim \tilde{\pi}$ and $\tilde{\pi}$ is the extended target measure described in [Lemma A.3](#). The constants C and K are given as

$$C = \sqrt{3}(\sqrt{L} \vee \sqrt{L}^{-1}), \quad K = L \left(1 + e^{L\eta^2} \left(\frac{\eta}{6} + \frac{\eta^2 L}{24} \right) \right) \left(1 + \frac{\eta L}{2\sqrt{\mu}} \right).$$

Note K converges to L as $\eta \rightarrow 0$.

Proof. See [Appendix B.5](#). \square

This is again a simple application of the triangle inequality for the concentration of π_Θ from [Proposition 2](#) and the convergence results for kinetic Langevin diffusions approximated by a second-order splitting scheme from [\[53\]](#).

4.4 Algorithmic Complexity and Acceleration

In this section, we show that the proposed underdamped diffusion accelerates the overdamped algorithms proposed for MMLE (i.e. IPLA [\[3\]](#) and PGD [\[47\]](#)) in the same way the KLMC methods accelerate overdamped samplers such as ULA. We note that we only discuss here the impact of dimension dependence and the target accuracy ε .

4.4.1 Algorithmic Complexity of KIPLMC1

To provide the algorithmic complexity of KIPLMC1, it is instructive to write the bound provided in [Theorem 1](#) free of constants that are not of interest to us:

$$\mathbb{E}[\|\theta_n - \bar{\theta}_*\|^2]^{1/2} \lesssim \left(1 - \frac{3\mu\eta}{4\gamma} \right)^n + \eta \sqrt{\frac{d_\theta + Nd_x}{N}} + \sqrt{\frac{d_\theta}{N}}, \quad (12)$$

where the notation \lesssim hides the constants that are not of interest⁴. In [\(12\)](#), we first set $N = \mathcal{O}(d_\theta \varepsilon^{-2})$ which ensures the last term in [\(12\)](#) is $\mathcal{O}(\varepsilon)$. Next, set $\eta = \mathcal{O}(\varepsilon d_x^{-1/2})$ which ensures that the second term is $\mathcal{O}(\varepsilon)$. It is then easy to see that $n = \tilde{\mathcal{O}}(\varepsilon^{-1} d_x^{1/2})$ steps are enough to obtain $\mathbb{E}[\|\theta_n - \bar{\theta}_*\|^2]^{1/2} \leq \varepsilon$.

Remark 1. *This dependency needs to be compared with IPLA and PGD. For the former, we note that our dependence to dimension for N is identical to IPLA and the dependence of the number of steps is significantly improved, i.e., we require $n = \tilde{\mathcal{O}}(d_x^{1/2} \varepsilon^{-1})$ whereas IPLA requires $n = \tilde{\mathcal{O}}(d_x \varepsilon^{-2})$ steps for the same accuracy. Regarding the latter method, PGD, our dependence to number of particles is different, as PGD requires $N = \mathcal{O}(d_x \varepsilon^{-2})$ (but this difference is a more general difference stemming from the different analysis techniques, as IPLA also has the same dependence as us to the number of particles N , see, e.g., [Corollary 8](#) and the subsequent discussion in [\[14\]](#)). However, in terms of the number of steps necessary to attain ε -error, we have the same improvement in dimension dependence in d_x and ε as we have compared to IPLA.*

4.4.2 Algorithmic Complexity of KIPLMC2

Using [Theorem 2](#), we can write for KIPLMC2 that

$$\mathbb{E}[\|\theta_n - \bar{\theta}_*\|^2]^{1/2} \lesssim \left(1 - \frac{\eta\mu}{3\gamma} \right)^{\frac{n}{2}} + \eta \sqrt{Nd_x + d_\theta} + \sqrt{\frac{d_\theta}{N}}, \quad (13)$$

Similarly to the analysis provided for KIPLMC1, we first set $N = \mathcal{O}(\varepsilon^{-2} d_\theta)$ to obtain $\mathcal{O}(\varepsilon)$ dependence in the last term of [\(13\)](#) and $\eta = \mathcal{O}(\varepsilon^2 (d_x d_\theta)^{-1/2})$ to obtain the same dependence in the second term of [\(13\)](#). Finally, setting $n = \tilde{\mathcal{O}}((d_x d_\theta)^{1/2} \varepsilon^{-2})$ brings us an accuracy of ε .

A few comments are in order for this complexity analysis for KIPLMC2.

⁴Note that we hide the dimension dependence of initial error $\mathbb{E}[\|Z_0 - Z^*\|^2]^{1/2}$ in this analysis. This dependence can be alleviated using a warm-start strategy in practice, e.g., running an optimiser first to initialise our algorithm, see, e.g., [\[14, Corollary 8\]](#).

	step count (n)	N	η
KIPLMC1	$\tilde{\mathcal{O}}(\sqrt{d_x}/\varepsilon)$	$\mathcal{O}(d_\theta/\varepsilon^2)$	$\mathcal{O}(\varepsilon/\sqrt{d_x})$
KIPLMC2	$\tilde{\mathcal{O}}(\sqrt{d_x d_\theta}/\varepsilon^2)$	$\mathcal{O}(d_\theta/\varepsilon^2)$	$\mathcal{O}(\varepsilon^2/\sqrt{d_x d_\theta})$
IPLA	$\tilde{\mathcal{O}}(d_x/\varepsilon^2)$	$\mathcal{O}(d_\theta/\varepsilon^2)$	$\mathcal{O}(\varepsilon^2/d_x)$
PGD	$\tilde{\mathcal{O}}(d_x/\varepsilon^2)$	$\mathcal{O}(d_x/\varepsilon^2)$	$\mathcal{O}(\varepsilon^2/d_x)$

Table 1: Comparison of orders required to achieve an error of order ε in W_2 , for step count, particle number N and step size η . The IPLA case holds for $\delta > 0$.

Remark 2. *In general, to avoid poor dependence on N , the error bounds of numerical discretisations must depend on L and μ with the same order. This ensures that the factors cancel out appropriately, preventing any undesirable effects. This is achieved by the analysis of the exponential integrator in [25] with a linear dependence on the condition number L/μ , thus our KIPLMC1 bound does not have a bad dependence to N . This enables us to obtain improved algorithmic complexity as discussed in Remark 1. However, for KIPLMC2, the OBABO scheme does not have this dependence on the condition number (see [53, Table 2]) under just H1 and H2. This results in a bound in Theorem 2 that grows as N grows. This is reflected therefore in the algorithmic complexity as KIPLMC2 theoretically requires $n = \tilde{\mathcal{O}}(\sqrt{d_x d_\theta} \varepsilon^{-2})$ steps to achieve ε error, compared to IPLA which requires $\tilde{\mathcal{O}}(d_x \varepsilon^{-2})$ steps. In this setting, the improvement (in dimension) only happens in the case where $d_\theta \leq d_x$, i.e., the dimension of parameter of the statistical model is less than the dimension of the latent variables.*

As summarised in Table 1 and Remark 2, the KIPLMC1 with a better order of convergence than the other algorithms, whilst the KIPLMC2 algorithm only has an improved rate when $d_\theta < d_x$. Indeed, the KIPLMC1 manages to fully exploit the accelerated convergence rate of the KLMC, due to the reduced sensitivity of the error on N . For a further discussion of a comparison of these scalings and those obtained by the Langevin samplers see [25, Sec. 3].

5 Experiments

In the following section a comparison will be made between the empirical results of KIPLMC1, KIPLMC2 algorithms, as well as, that of MPGD from [49]. We note that, in [49], the MPGD is not solely the discretisation of the KIPLD-like SDE using the exponential integrator which the authors of [49] found unstable. The MPGD proposed by [49] includes a *gradient correction* term. For a fair comparison, we implement both MPGD with gradient correction (which is referred to as MPGD) and MPGD without the gradient correction which we refer to as momentum particle gradient descent with no correction (MPGDnc). Our KIPLMC1 method is comparable to MPGDnc rather than MPGD which includes a gradient correction step, making theoretical analysis nontrivial.

In the following sections, we will consider three examples: (i) Bayesian logistic regression for synthetic data, (ii) Bayesian logistic regression on Wisconsin Cancer dataset, and (iii) a Bayesian Neural Network (BNN) example as a more challenging, non-convex example.

5.1 Bayesian Logistic Regression on Synthetic Data

We follow the experimental setting in [47] and [3] and start with comparisons between algorithms on a synthetic dataset for which we know the true solution. More precisely, consider the Bayesian logistic regression model

$$p_\theta(x) = \mathcal{N}(x; \theta, \sigma^2 I_{d_x}), \quad p(y|x) = \prod_{j=1}^{d_y} s(v_j^\top x)^{y_j} (1 - s(v_j^\top x))^{1-y_j}.$$

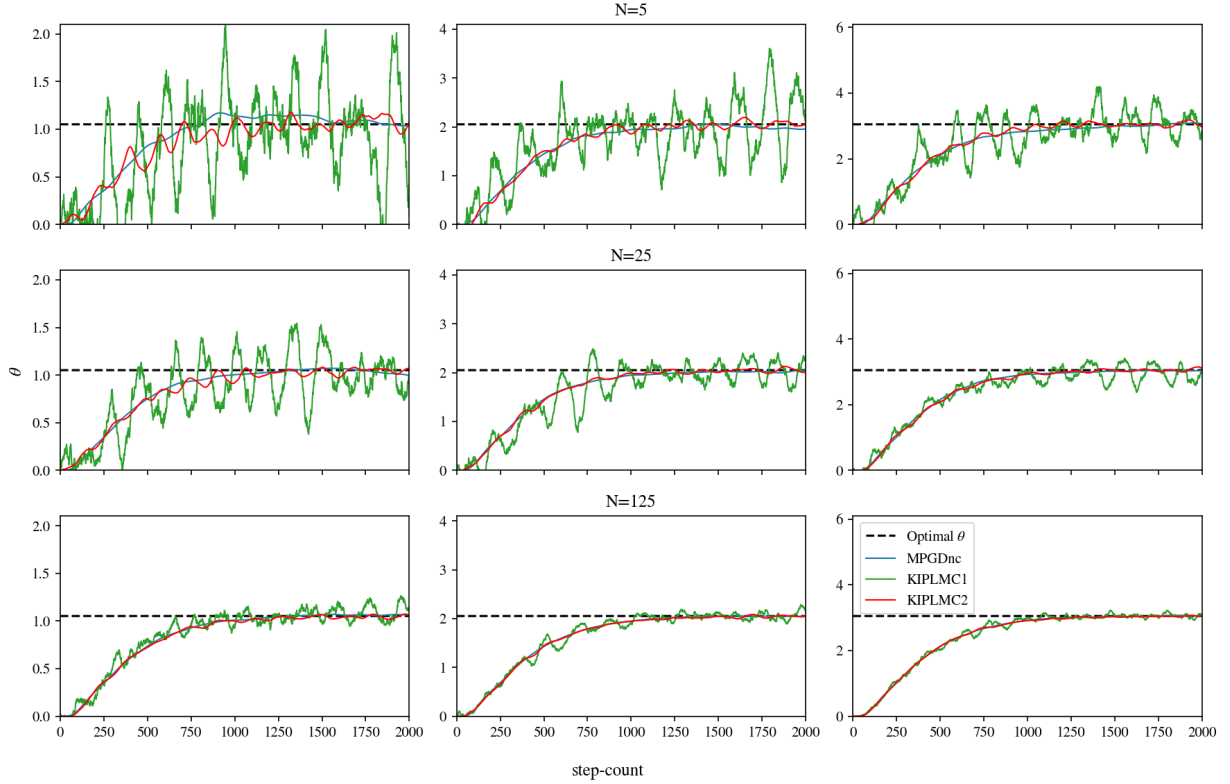


Figure 1: **Parameter estimate comparison.** We compare the performance of the MPGDnc, KIPLMC1, and KIPLMC2 algorithms on the synthetic dataset with true $\bar{\theta}_* \in [1, 2, 3]$. We observe the desired convergence of behaviours for larger values of N . For all the algorithms, with the chosen γ , we observe momentum effects, which extend to the noise, as can be seen in the oscillations in the low particle number regimes. In this example $d_x = d_\theta = 3$, $d_y = 500$ and $\gamma = 1.2$. Z_0 is set as δ , the point measure on the origin.

Here $s(u) = e^u / (1 + e^u)$ is the logistic function and v_j , $j \in [d_y]$ are the set of d_x -dimensional covariates with corresponding responses $y_j \in \{0, 1\}$. σ is given and fixed throughout. We generate a synthetic set of covariates, $\{v_j\}_{j=1}^{d_y} \subset \mathbb{R}^{d_x}$, from which are simulated a synthetic set of observations $y_j | \bar{\theta}_*, x, v_j$, for fixed $\bar{\theta}_*$, via a Bernoulli random variable with probability $s(v_j^\top x)$. The algorithm is tested on the recovery of this value of $\bar{\theta}_*$.

The marginal likelihood is given as,

$$p_\theta(y) = \frac{1}{(2\pi\sigma^2)^{d_x/2}} \int_{\mathbb{R}^{d_x}} \left(\prod_{j=1}^{d_y} s(v_j^\top x)^{y_j} (1 - s(v_j^\top x))^{1-y_j} \right) \exp\left(-\frac{\|x - \theta\|^2}{2\sigma^2}\right) dx.$$

From this it easy to see that the gradients of U are given as,

$$\nabla_\theta U(\theta, x) = -\frac{x - \theta}{\sigma^2}, \quad \nabla_x U(\theta, x) = \frac{x - \theta}{\sigma^2} - \sum_{j=1}^{d_y} (y_j - s(v_j^\top x)) v_j. \quad (14)$$

Remark 3 (On H1 and H2). We will discuss this problem and our assumptions. From (14) it is quite straightforward to observe that,

$$\begin{aligned} \|\nabla U(z) - \nabla U(z')\| &\leq \frac{2}{\sigma^2} (\|x - x'\| + \|\theta - \theta'\|) + \sum_{j=1}^{d_y} |s(v_j^\top x) - s(v_j^\top x')| \|v_j\| \\ &\leq \left(\frac{2}{\sigma^2} + \frac{1}{4} \sum_{j=1}^{d_y} \|v_j\|^2\right) \|z - z'\|. \end{aligned}$$

This follows from the fact that the logistic function is Lipschitz continuous with constant 1/4 [3]. Hence, H2 is satisfied.

For H1, consider

$$\nabla^2 U(z) = \frac{1}{\sigma^2} \begin{pmatrix} I_{d_\theta} & -I_{d_x} \\ -I_{d_x} & I_{d_\theta} \end{pmatrix} + \sum_{j=1}^{d_y} s(v_j^\top x)(1 - s(v_j^\top x)) v_j \otimes v_j.$$

The sum is positive definite and the matrix was shown by [47] to have $2d_\theta$ positive eigenvalues and so it follows that $\nabla^2 U$ is positive definite. Hence U is strictly convex and in theory no lower bound for strong convexity constant exists. We show however this is not a problem for our practical implementations.

In Fig. 1 we can see the difference in the behaviours between the algorithms. Most notably, the KIPLMC2 algorithm exhibits comparable levels of variance as the MPGDnc algorithm in the θ -dimension, whilst the KIPLMC1 algorithm has much greater variance (roughly 100 times greater). It is interesting to note that the KIPLMC2 algorithm preserves many theoretical properties of the KIPLMC1 algorithm, with empirical variance reduction properties. As N grows the θ iterates concentrate onto the MMLE $\hat{\theta}_*$ for all algorithms. This behaviour can be seen in more detail in Fig. 2 (b), in which we can observe the variance changing with rate $\mathcal{O}(1/N)$. Further, we make a comparison of the performance of the MPGDnc and KIPLMC2 in Fig. 2 (a) with the Area Below the Curve (ABC) metric (see C.1 for more detail). This metric is a signed, weighted difference between the performances of the two algorithms: the higher the value, the better KIPLMC2 performs compared to MPGDnc; 0 is when they perform the same. We observe that the best comparative performance for the KIPLMC2 algorithm arises in the edge cases where we have large step-size and small particle number.

Note that the momentum effects of the KIPLMC1 and KIPLMC2 algorithms has been dampened through a specific choice of γ . In training it was observed that the convergence rate is very sensitive to the choice of γ , where choices too small exhibit large momentum effects and too large lead to slow convergence. The choice of γ here is far from optimal, but allows us to observe the strength of the proposed algorithms.

5.2 Wisconsin Cancer Data

We follow again an experimental procedure that is similar to the one outlined in [47] and [3] and make comparisons between the algorithms on a more realistic dataset: the Wisconsin Cancer Data. Again, we use the logistic regression LVM model, outlined above. This task is a binary classification, to determine from 9 features gathered from tumors and 693 data points labelled as either benign or malignant. The latent variables correspond to the features extracted from the data. The task in this case is to seek to model the behaviour as accurately as possible through the logistic regression LVM.

For this setup we define our probability model as,

$$p_\theta(x) = \mathcal{N}(x; \theta \mathbb{1}_{d_x}, 5I_{d_x})$$

and the likelihood as,

$$p(y|x) = \prod_{j=1}^{d_y} s(v_j^\top x)^{y_j} (1 - s(v_j^\top x))^{1-y_j}.$$

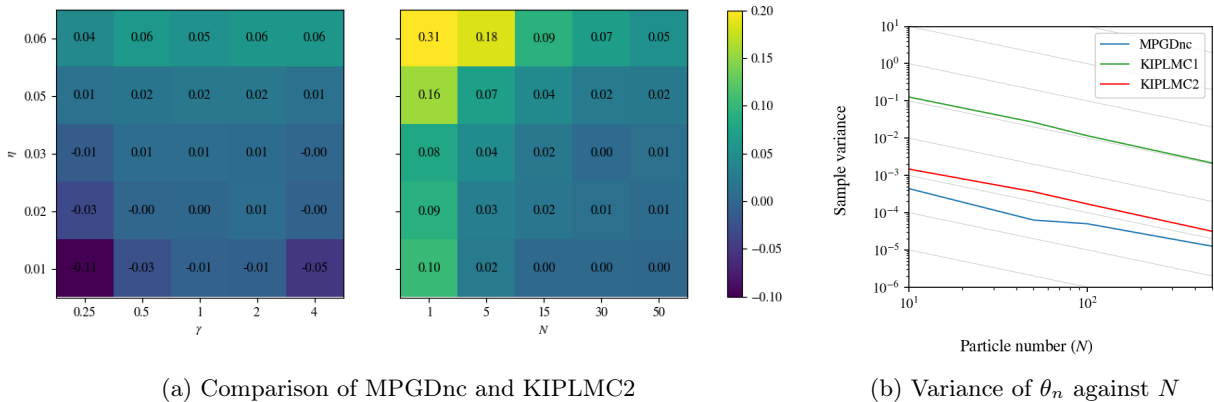


Figure 2: **Comparison over hyper-parameters.** These figures compare the performance of MPGDnc with the proposed algorithms. (a) shows the Area Between the Curve (ABC) values between MPGDnc and KIPLMC2 for a variety of hyper-parameter combinations. (discussed in C.1). (b) makes a comparison over 20 Monte Carlo simulations of the algorithms’ sample variances, using the last 500 steps of each simulation. The scales are logarithmic and grid-lines corresponding to $\frac{1}{N}$ are provided to highlight the rate of convergence. Where not specified otherwise, simulations are run with $\eta = 0.01$, $\gamma = 0.7$ and $N = 50$.

Note that the parameter θ is a scalar in this case, hence, this turns out to be a simplified version of the setup described above and so the discussion in Remark 3 is still valid. As opposed to the previous case with synthetic data, here we consider a real dataset, thus we do not have access to the true dataset. Hence, there is no comparison to a $\hat{\theta}_*$, but we can see that different algorithms attain similar values as the estimate of this minimum.

Most notably in this experiment, we can observe in Fig. 3 the importance of the discretisation KIPLMC2. In particular, this algorithm displays great stability w.r.t. the choice of the step-size. For small values of the step-size, the MPGDnc algorithm performs with the lowest variance in all cases where it converges, until it explodes where step-sizes become too large (for more detail see C.2). This is remedied by implementing a gradient correction trick, discussed in [49], though we show how the algorithm performs without for a comparison with KIPLMC1. Again, we note that the KIPLMC1 algorithm exhibits more variance in the θ estimation than the KIPLMC2 and MPGD algorithms. This is typically an advantage when working with convex problems, but this “sticky” behaviour might prove detrimental in the non-convex case [38, 3]. The injection of noise into the parameter estimation may help the method to escape local minima [1]. In these algorithms one can observe the strength of the KIPLMC2 algorithm, with fast convergence and smoother paths. The latter observation may be related to the differing orders of the algorithms in [53] and [25].

5.3 Bayesian Neural Network

Similarly to [47, 49] we also consider a Bayesian Neural Network (BNN) example to perform character classification on the MNIST dataset. This dataset and model provide a more challenging problem for the 1 and 2 algorithms as the posteriors are known to be multi-modal. MNIST contains 70’000 28×28 grey-scale images $\{f_i\}_{i=1}^{70000} \subset \mathbb{R}^{784}$. However, to avoid issues of high dimensionality, we consider a normalised subset of 1’000 characters containing only images of fours and nines, whose similarity should pose a challenge.

Following [47] we employ a two layer BNN with tanh activation function, softmax output layer and 40 dimensional latent space. i.e. we consider the probability of the data labels l to be conditionally independent,

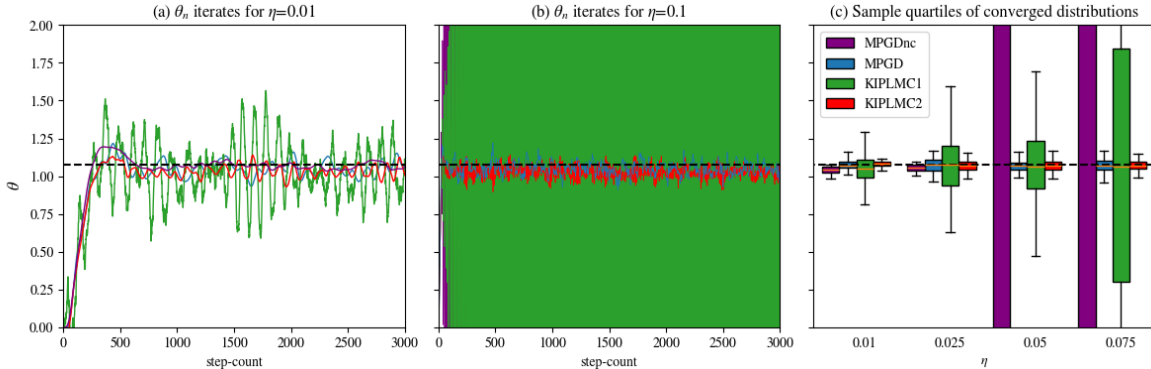


Figure 3: **Wisconsin Dataset.** The performance of MPGD, MPGDnc, KIPLMC1 and KIPLMC2 algorithms are compared on a logistic regression experiment for the Wisconsin Cancer Dataset. In (a), we show the behaviour of the θ_n iterates for the small step-size of $\eta = 0.01$, where all algorithms converge as desired. (b) shows the behaviour θ_n iterates for a step-size where some algorithms explode. In (c) we compare the distributions of the algorithms over different step-sizes. MPGDnc is the MPGD algorithm without gradient correction. The particle number, is chosen to be $N = 50$ and $\gamma = 1.2$.

given the features f and the weights $x = (w, v)$, with model,

$$p(l|f, x) \propto \exp \left(\sum_{j=1}^{40} v_{lj} \tanh \left(\sum_{i=1}^{784} w_{ji} f_i \right) \right),$$

where $w \in \mathbb{R}^{40 \times 784}$, $v \in \mathbb{R}^{2 \times 40}$. Consider the priors on the weights to be without bias and Gaussian: $w \sim \mathcal{N}(0, e^{2\alpha} \mathbb{I})$ and $v \sim \mathcal{N}(0, e^{2\beta} \mathbb{I})$. Rather than assigning these priors, we learn the parameters $\theta = (\alpha, \beta) \in \mathbb{R}^2$ jointly with the latent variables x . Hence, the model's density is given as

$$p_{\theta}(x, \{f_i\}_{i=1}^{1000}) = \mathcal{N}(w; 0, e^{2\alpha} \mathbb{I}) \mathcal{N}(v; 0, e^{2\beta} \mathbb{I}) \prod_{i=1}^{1000} p(l|f_i, x).$$

Notice again that we are unable to confirm the validity of our assumptions. We will employ autograd methods from the JAX library to compute the gradients.

In Fig. 4 we make a comparison between the different algorithms over one run, comparing the log predictive point-wise density (LPPD), relative error and the density of the last estimate of w . The LPPD is the average log-likelihood assigned to the correct response, whilst the relative error is given as the accuracy of prediction on a test set (see C.3 for more detail). Observe the improved behaviour of the KIPLMC2 algorithm in LPPD (a), comparable behaviour in relative error (b). Note however that the KIPLMC2 algorithm converges to a different solution than all other algorithms in our simulations.

6 Conclusions

This paper extends a line of work on interacting particle, and more generally diffusion-based, algorithms for maximum marginal likelihood estimation. This paper has focused on considering alternatives to the IPSs proposed by [47, 3, 49] for the MMLE problem by considering an accelerated variant. We have shown that we can leverage the existing literature on underdamped Langevin diffusion for sampling [25, 20, 53, 51] to produce two algorithms with greater stability, added smoothness and exponential convergence, which concentrate onto the MMLE with quantitative nonasymptotic bounds on the estimation error as measured by

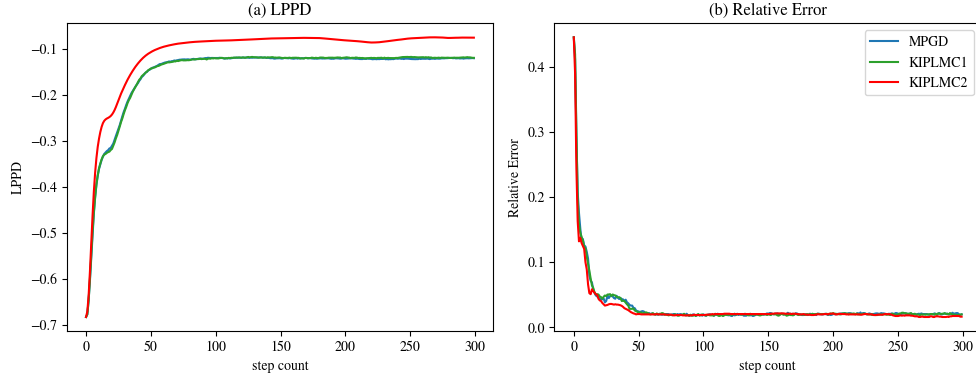


Figure 4: **Bayesian Neural Network.** (a) LPPD estimates as a function of step count, and (b) the relative error (for a discussion of these metrics see C.3). All algorithms hover around an relative error of 0.02 when converged. Shown are the averaged behaviour over 10 simulations, which were all run with $N = 100$, $\gamma = 1.9$ and $\eta = 0.015$.

$\mathbb{E}[\|\theta_n - \bar{\theta}_*\|^2]^{1/2}$. In particular, we show that the KIPLMC1 does attain an accelerated error rate for attaining an error of order ε after $\tilde{\mathcal{O}}(\sqrt{d_x}\varepsilon^{-1})$ steps, compared to the IPLA and PGD which require $\tilde{\mathcal{O}}(d_x\varepsilon^{-2})$ steps.

Proposed algorithms within this manuscript are both based on a momentum-based diffusion - which can both be seen as a relaxation of the friction of the IPLA in [3] or as a noised version of the MIPGD in [49]. Empirically, the algorithms perform well compared to the MIPGD (with equal choice of step-sizes and friction coefficients). Specifically, the induced noise should improve guarantees in the non-convex setting, as discussed in [3, 57, 1]. The results presented here hold under assumptions of gradient-Lipschitzness and strong log-concavity, however, following the work done in the analysis of Langevin diffusions under nonconvexity and without global Lipschitz continuity (see, e.g., [71, 1, 44]), it is possible to extend these results to these cases, which is left for future work. Another interesting direction is to consider the setting in [36], using an accelerated algorithm for the high-dimensional linear models. Our methods can also be adapted to solving linear inverse problems as done by [5]. Similar ideas can be considered within the setting of Stein variational gradient descent as done in [63].

Acknowledgements

We would like to thank Juan Kuntz and Paula Cordero Encinar for their insightful comments and suggestions.

PVO is supported by the EPSRC through the Modern Statistics and Statistical Machine Learning (StatML) CDT programme, grant no. EP/S023151/1.

References

- [1] Ö. Deniz Akyildiz and Sotirios Sabanis. Nonasymptotic analysis of stochastic gradient hamiltonian monte carlo under local conditions for nonconvex optimization. *Journal of Machine Learning Research*, 25(113):1–34, 2024. Cited on pages 5, 10, 11, 17, and 19.
- [2] Ö. Deniz Akyildiz, Dan Crisan, and Joaquín Míguez. Parallel sequential Monte Carlo for stochastic gradient-free nonconvex optimization. *Statistics and Computing*, 30(6):1645–1663, 2020. Cited on page 2.
- [3] Ö Deniz Akyildiz, Francesca Romana Crucinio, Mark Girolami, Tim Johnston, and Sotirios Sabanis. Interacting particle Langevin algorithm for maximum marginal likelihood estimation. *arXiv preprint arXiv:2303.13429*, 2023. Cited on pages 2, 3, 6, 7, 13, 14, 16, 17, 18, 19, and 29.

- [4] Ö. Deniz Akyildiz, Michela Ottobre, and Iain Souttar. A multiscale perspective on maximum marginal likelihood estimation. *arXiv preprint arXiv:2406.04187*, 2024. Cited on page 2.
- [5] Ömer Deniz Akyildiz, Connor Duffin, Sotirios Sabanis, and Mark Girolami. Statistical finite elements via langevin dynamics. *SIAM/ASA Journal on Uncertainty Quantification*, 10(4):1560–1585, 2022. Cited on page 19.
- [6] Yves F. Atchadé, Gersende Fort, and Eric Moulines. On perturbed proximal gradient algorithms. *Journal of Machine Learning Research*, 18(10):1–33, 2017. URL <http://jmlr.org/papers/v18/15-038.html>. Cited on pages 2 and 6.
- [7] José M Bernardo and Adrian FM Smith. *Bayesian theory*, volume 405. John Wiley & Sons, 2009. Cited on page 2.
- [8] P. Billingsley. *Probability and Measure*. Wiley Series in Probability and Statistics. Wiley, 1995. ISBN 9780471007104. URL <https://books.google.co.uk/books?id=z39jQgAACAAJ>. Cited on page 10.
- [9] David M Blei, Andrew Y Ng, and Michael I Jordan. Latent Dirichlet allocation. *Journal of Machine Learning Research*, 3(Jan):993–1022, 2003. Cited on page 1.
- [10] James G Booth and James P Hobert. Maximizing generalized linear mixed model likelihoods with an automated Monte Carlo EM algorithm. *Journal of the Royal Statistical Society: Series B (Statistical Methodology)*, 61(1):265–285, 1999. Cited on page 2.
- [11] Anastasia Borovykh, Nikolas Kantas, Panos Parpas, and Greg Pavliotis. Optimizing interacting Langevin dynamics using spectral gaps. In *Proceedings of the 38th International Conference on Machine Learning (ICML 2021)*, 2021. Cited on page 2.
- [12] Nicolas Brosse, Alain Durmus, Éric Moulines, and Sotirios Sabanis. The tamed unadjusted Langevin algorithm. *Stochastic Processes and their Applications*, 129(10):3638–3663, 2019. Cited on page 4.
- [13] Olivier Cappé, Arnaud Doucet, Marc Lavielle, and Eric Moulines. Simulation-based methods for blind maximum-likelihood filter identification. *Signal Processing*, 73(1-2):3–25, 1999. Cited on page 2.
- [14] Rocco Caprio, Juan Kuntz, Samuel Power, and Adam M. Johansen. Error bounds for particle gradient descent, and extensions of the log-sobolev and talagrand inequalities, 2024. Cited on pages 2 and 13.
- [15] Gilles Celeux. The SEM algorithm: a probabilistic teacher algorithm derived from the em algorithm for the mixture problem. *Computational Statistics Quarterly*, 2:73–82, 1985. Cited on page 2.
- [16] Gilles Celeux and Jean Diebolt. A stochastic approximation type EM algorithm for the mixture problem. *Stochastics: An International Journal of Probability and Stochastic Processes*, 41(1-2):119–134, 1992. Cited on page 2.
- [17] KS Chan and Johannes Ledolter. Monte Carlo EM estimation for time series models involving counts. *Journal of the American Statistical Association*, 90(429):242–252, 1995. Cited on page 2.
- [18] Huy N Chau and Miklós Rásonyi. Stochastic gradient hamiltonian monte carlo for non-convex learning. *Stochastic Processes and their Applications*, 149:341–368, 2022. Cited on page 5.
- [19] Xiang Cheng, Niladri S Chatterji, Yasin Abbasi-Yadkori, Peter L Bartlett, and Michael I Jordan. Sharp convergence rates for Langevin dynamics in the nonconvex setting. *arXiv preprint arXiv:1805.01648*, 2018. Cited on page 5.
- [20] Xiang Cheng, Niladri S Chatterji, Peter L Bartlett, and Michael I Jordan. Underdamped Langevin MCMC: A non-asymptotic analysis. In *Conference On Learning Theory*, pages 300–323, 2018. Cited on pages 3, 5, 7, 8, and 18.

- [21] Sinho Chewi, Murat A Erdogdu, Mufan Li, Ruoqi Shen, and Shunshi Zhang. Analysis of Langevin Monte Carlo from Poincare to Log-Sobolev. In *Conference on Learning Theory*, pages 1–2. PMLR, 2022. Cited on page 4.
- [22] Arnak Dalalyan. Further and stronger analogy between sampling and optimization: Langevin monte carlo and gradient descent. In *Conference on Learning Theory*, pages 678–689, 2017. Cited on pages 2 and 4.
- [23] Arnak S Dalalyan. Theoretical guarantees for approximate sampling from smooth and log-concave densities. *Journal of the Royal Statistical Society: Series B (Statistical Methodology)*, 79(3):651–676, 2017. Cited on pages 2, 6, and 10.
- [24] Arnak S Dalalyan and Avetik Karagulyan. User-friendly guarantees for the Langevin Monte Carlo with inaccurate gradient. *Stochastic Processes and their Applications*, 129(12):5278–5311, 2019. Cited on pages 4 and 10.
- [25] Arnak S Dalalyan and Lionel Riou-Durand. On sampling from a log-concave density using kinetic langevin diffusions. *Bernoulli*, 26(3):1956–1988, 2020. Cited on pages 2, 3, 4, 5, 7, 8, 9, 12, 14, 17, 18, 26, and 29.
- [26] Valentin De Bortoli, Alain Durmus, Marcelo Pereyra, and Ana F Vidal. Efficient stochastic optimisation by unadjusted langevin monte carlo. *Statistics and Computing*, 31(3):1–18, 2021. Cited on pages 2 and 6.
- [27] Arthur P Dempster, Nan M Laird, and Donald B Rubin. Maximum likelihood from incomplete data via the em algorithm. *Journal of the Royal Statistical Society: Series B (Methodological)*, 39(1):1–22, 1977. Cited on pages 1 and 2.
- [28] J Diebolt and E HS Ip. A stochastic EM algorithm for approximating the maximum likelihood estimate. In W. R. Gilks, S. T. Richardson, and D. J. Spiegelhalter, editors, *Markov Chain Monte Carlo in Practice*. CRC Publishers, 1996. Cited on page 2.
- [29] Randal Douc, Eric Moulines, and David Stoffer. *Nonlinear time series: Theory, methods and applications with R examples*. CRC press, 2014. Cited on page 6.
- [30] Jin-Chuan Duan, Andras Fulop, and Yu-Wei Hsieh. Maximum likelihood estimation of latent variable models by SMC with marginalization and data cloning. *USC-INET Research Paper*, (17-27), 2017. Cited on page 2.
- [31] Alain Durmus and Eric Moulines. Nonasymptotic convergence analysis for the unadjusted Langevin algorithm. *The Annals of Applied Probability*, 27(3):1551–1587, 2017. Cited on pages 2, 4, 6, and 10.
- [32] Alain Durmus and Eric Moulines. High-dimensional Bayesian inference via the unadjusted Langevin algorithm. *Bernoulli*, 25(4A):2854–2882, 2019. Cited on pages 2, 4, 6, and 7.
- [33] Alain Durmus, Szymon Majewski, and Błażej Miasojedow. Analysis of Langevin Monte Carlo via convex optimization. *Journal of Machine Learning Research*, 20(1):2666–2711, 2019. Cited on pages 2 and 4.
- [34] Andreas Eberle, Arnaud Guillin, and Raphael Zimmer. Couplings and quantitative contraction rates for Langevin dynamics. *The Annals of Probability*, 47(4):1982–2010, 2019. Cited on page 28.
- [35] Paula Cordero Encinar, Francesca R Crucinio, and O. Deniz Akyildiz. Proximal Interacting Particle Langevin Algorithms. *arXiv preprint arXiv:2406.14292*, 2024. Cited on page 2.
- [36] Zhou Fan, Leying Guan, Yandi Shen, and Yihong Wu. Gradient flows for empirical bayes in high-dimensional linear models. *arXiv preprint arXiv:2312.12708*, 2023. Cited on page 19.
- [37] Carlo Gaetan and Jian-Feng Yao. A multiple-imputation Metropolis version of the EM algorithm. *Biometrika*, 90(3):643–654, 2003. Cited on page 2.

- [38] Xuefeng Gao, Mert Gürbüzbalaban, and Lingjiong Zhu. Global convergence of stochastic gradient hamiltonian monte carlo for nonconvex stochastic optimization: Nonasymptotic performance bounds and momentum-based acceleration. *Operations Research*, 70(5):2931–2947, 2022. Cited on pages 5 and 17.
- [39] Sara Grassi and Lorenzo Pareschi. From particle swarm optimization to consensus based optimization: stochastic modeling and mean-field limit. *Mathematical Models and Methods in Applied Sciences*, 31(08):1625–1657, 2021. Cited on page 2.
- [40] Peter D Hoff, Adrian E Raftery, and Mark S Handcock. Latent space approaches to social network analysis. *Journal of the American Statistical association*, 97(460):1090–1098, 2002. Cited on page 1.
- [41] Chii-Ruey Hwang. Laplace’s method revisited: weak convergence of probability measures. *The Annals of Probability*, pages 1177–1182, 1980. Cited on pages 6 and 11.
- [42] Eric Jacquier, Michael Johannes, and Nicholas Polson. MCMC maximum likelihood for latent state models. *Journal of Econometrics*, 137(2):615–640, 2007. Cited on page 2.
- [43] Adam M Johansen, Arnaud Doucet, and Manuel Davy. Particle methods for maximum likelihood estimation in latent variable models. *Statistics and Computing*, 18(1):47–57, 2008. Cited on page 2.
- [44] Tim Johnston, Iosif Lytras, and Sotirios Sabanis. Kinetic langevin mcmc sampling without gradient lipschitz continuity—the strongly convex case. *Journal of Complexity*, 2024. Cited on pages 19 and 29.
- [45] Tim Johnston, Nikolaos Makras, and Sotirios Sabanis. Taming the interacting particle langevin algorithm—the superlinear case. *arXiv preprint arXiv:2403.19587*, 2024. Cited on pages 2 and 10.
- [46] James Kennedy and Russell Eberhart. Particle swarm optimization. In *Proceedings of ICNN’95-international conference on neural networks*, volume 4, pages 1942–1948. IEEE, 1995. Cited on page 2.
- [47] Juan Kuntz, Jen Ning Lim, and Adam M Johansen. Particle algorithms for maximum likelihood training of latent variable models. In *International Conference on Artificial Intelligence and Statistics*, pages 5134–5180. PMLR, 2023. Cited on pages 2, 3, 6, 13, 14, 16, 17, 18, 30, and 31.
- [48] Kenneth Lange. A gradient algorithm locally equivalent to the em algorithm. *Journal of the Royal Statistical Society: Series B (Methodological)*, 57(2):425–437, 1995. Cited on page 2.
- [49] Jen Ning Lim, Juan Kuntz, Samuel Power, and Adam M Johansen. Momentum particle maximum likelihood. In *Proceedings of 41st International Conference on Machine Learning (ICML)*, volume 235, 2024. Cited on pages 2, 3, 6, 7, 14, 17, 18, 19, and 30.
- [50] Chuanhai Liu and Donald B Rubin. The ecme algorithm: a simple extension of em and ecm with faster monotone convergence. *Biometrika*, 81(4):633–648, 1994. Cited on page 2.
- [51] Yi-An Ma, Niladri S. Chatterji, Xiang Cheng, Nicolas Flammarion, Peter L. Bartlett, and Michael I. Jordan. Is there an analog of Nesterov acceleration for gradient-based MCMC? *Bernoulli*, 27(3):1942 – 1992, 2021. doi: 10.3150/20-BEJ1297. URL <https://doi.org/10.3150/20-BEJ1297>. Cited on pages 2, 5, 7, and 18.
- [52] Xiao-Li Meng and Donald B Rubin. Maximum likelihood estimation via the ecm algorithm: A general framework. *Biometrika*, 80(2):267–278, 1993. Cited on page 2.
- [53] Pierre Monmarché. High-dimensional MCMC with a standard splitting scheme for the underdamped Langevin diffusion. *Electronic Journal of Statistics*, 15(2):4117–4166, 2021. Cited on pages 3, 7, 8, 9, 13, 14, 17, 18, and 30.
- [54] Edward Nelson. *Dynamical Theories of Brownian Motion*. Princeton University Press, 1967. ISBN 9780691079509. URL <http://www.jstor.org/stable/j.ctv15r57jg.1>. Cited on page 5.

- [55] Grigorios A. Pavliotis. *Stochastic processes and applications: Diffusion Processes, the Fokker-Planck and Langevin equations*. Springer, 2014. Cited on pages 4, 5, 10, and 27.
- [56] René Pinnau, Claudia Totzeck, Oliver Tse, and Stephan Martin. A consensus-based model for global optimization and its mean-field limit. *Mathematical Models and Methods in Applied Sciences*, 27(01):183–204, 2017. Cited on page 2.
- [57] Maxim Raginsky, Alexander Rakhlin, and Matus Telgarsky. Non-convex learning via Stochastic Gradient Langevin Dynamics: a nonasymptotic analysis. In *Conference on Learning Theory*, pages 1674–1703, 2017. Cited on page 19.
- [58] Christian P Robert and George Casella. *Monte Carlo statistical methods*. John Wiley & Sons, 2004. Cited on page 4.
- [59] Gareth O Roberts and Osnat Stramer. Langevin diffusions and metropolis-hastings algorithms. *Methodology and computing in applied probability*, 4(4):337–357, 2002. Cited on page 4.
- [60] Gareth O Roberts, Richard L Tweedie, et al. Exponential convergence of Langevin distributions and their discrete approximations. *Bernoulli*, 2(4):341–363, 1996. Cited on page 4.
- [61] Filippo Santambrogio. Optimal transport for applied mathematicians. *Birkäuser, NY*, 55(58-63):94, 2015. Cited on page 11.
- [62] Adrien Saumard and Jon A Wellner. Log-concavity and strong log-concavity: a review. *Statistics surveys*, 8:45, 2014. Cited on page 29.
- [63] Louis Sharrock, Daniel Dodd, and Christopher Nemeth. Tuning-free maximum likelihood training of latent variable models via coin betting. In *International Conference on Artificial Intelligence and Statistics*, pages 1810–1818. PMLR, 2024. Cited on page 19.
- [64] Robert P Sherman, Yu-Yun K Ho, and Siddhartha R Dalal. Conditions for convergence of Monte Carlo EM sequences with an application to product diffusion modeling. *The Econometrics Journal*, 2(2):248–267, 1999. Cited on page 2.
- [65] Paris Smaragdis, Bhiksha Raj, and Madhusudana Shashanka. A probabilistic latent variable model for acoustic modeling. *Advances in Models for Acoustic Processing Workshop, NIPS*, 148:8–1, 2006. Cited on page 1.
- [66] Arnaud Vadeboncoeur, Ö. Deniz Akyildiz, Ieva Kazlauskaitė, Mark Girolami, and Fehmi Cirak. Fully probabilistic deep models for forward and inverse problems in parametric pdes. *Journal of Computational Physics*, 491:112369, 2023. ISSN 0021-9991. doi: <https://doi.org/10.1016/j.jcp.2023.112369>. URL <https://www.sciencedirect.com/science/article/pii/S0021999123004643>. Cited on page 1.
- [67] Santosh Vempala and Andre Wibisono. Rapid convergence of the unadjusted Langevin algorithm: Isoperimetry suffices. *Advances in Neural Information Processing Systems*, 32, 2019. Cited on page 4.
- [68] Greg CG Wei and Martin A Tanner. A Monte Carlo implementation of the EM algorithm and the poor man’s data augmentation algorithms. *Journal of the American Statistical Association*, 85(411):699–704, 1990. Cited on page 2.
- [69] Nick Whiteley, Annie Gray, and Patrick Rubin-Delanchy. Statistical exploration of the manifold hypothesis. *arXiv preprint arXiv:2208.11665*, 2022. Cited on page 1.
- [70] Tatiana Xifara, Chris Sherlock, Samuel Livingstone, Simon Byrne, and Mark Girolami. Langevin diffusions and the metropolis-adjusted langevin algorithm. *Statistics & Probability Letters*, 91:14–19, 2014. Cited on page 4.

- [71] Ying Zhang, Ö. Deniz Akyildiz, Theodoros Damoulas, and Sotirios Sabanis. Nonasymptotic estimates for stochastic gradient langevin dynamics under local conditions in nonconvex optimization. *Applied Mathematics & Optimization*, 87(2):25, 2023. Cited on pages [10](#), [11](#), and [19](#).

Appendix

A Preliminary results

Lemma A.1 (KIPLD as an underdamped Langevin Diffusion). *The KIPLD diffusion can be equivalently written as a single $d_\theta + Nd_x$ -dimensional underdamped Langevin diffusion given by*

$$\begin{aligned} d\mathbf{Z}_t &= \bar{\mathbf{V}}_t^z dt, \\ d\bar{\mathbf{V}}_t^z &= -\gamma \bar{\mathbf{V}}_t^z dt - \nabla_z \bar{U}_N(\mathbf{Z}_t) dt + \sqrt{\frac{2\gamma}{N}} d\mathbf{B}_t, \end{aligned} \quad (15)$$

where $\mathbf{Z}_t^i = N^{-1/2} \mathbf{X}_t^i$ for $i = 1, \dots, N$, $\mathbf{Z}_t = (\boldsymbol{\theta}_t, \mathbf{Z}_t^1, \dots, \mathbf{Z}_t^N)^\top \in \mathbb{R}^{d_\theta + Nd_x}$, $\bar{\mathbf{V}}_t^{z^i} = N^{-1/2} \mathbf{V}_t^{z^i}$ and $\bar{\mathbf{V}}_t^z = (\mathbf{V}_t^\theta, \bar{\mathbf{V}}_t^{z^1}, \dots, \bar{\mathbf{V}}_t^{z^N})^\top \in \mathbb{R}^{d_\theta + Nd_x}$, $(\mathbf{B}_t)_{t \geq 0}$ is a $\mathbb{R}^{d_\theta + Nd_x}$ -valued Brownian motion, and

$$\bar{U}_N(\theta, z_1, \dots, z_N) := \frac{1}{N} \sum_{i=1}^N U(\theta, \sqrt{N} z_i).$$

Proof. Recall the KIPLD system:

$$\begin{aligned} d\boldsymbol{\theta}_t &= \mathbf{V}_t^\theta dt \\ d\mathbf{X}_t^i &= \mathbf{V}_t^{x^i} dt, \quad \text{for } i = 1, \dots, N \\ d\mathbf{V}_t^\theta &= -\gamma \mathbf{V}_t^\theta dt - \frac{1}{N} \sum_{i=1}^N \nabla_\theta U(\boldsymbol{\theta}_t, \mathbf{X}_t^i) dt + \sqrt{\frac{2\gamma}{N}} d\mathbf{B}_t^0 \\ d\mathbf{V}_t^{x^i} &= -\gamma \mathbf{V}_t^{x^i} dt - \nabla_x U(\boldsymbol{\theta}_t, \mathbf{X}_t^i) dt + \sqrt{2\gamma} d\mathbf{B}_t^i, \quad \text{for } i \in [N] \end{aligned}$$

We note now that, below, we generically use the gradient functions $\nabla_\theta U(\theta, x) : \mathbb{R}^{d_\theta} \times \mathbb{R}^{d_x} \rightarrow \mathbb{R}^{d_\theta}$ and $\nabla_x U(\theta, x) : \mathbb{R}^{d_\theta} \times \mathbb{R}^{d_x} \rightarrow \mathbb{R}^{d_x}$ even though their arguments may change. In other words, below $\nabla_\theta U(\theta, x)$ denotes the gradient of U with respect to its first argument and $\nabla_x U(\theta, x)$ denotes the gradient of U with respect to its second argument.

Let us introduce the following function:

$$U_N(\theta, x) = U(\theta, \sqrt{N}x),$$

where we note that the (full) gradient is given as,

$$\nabla U_N(\theta, x) = \begin{pmatrix} \nabla_\theta U(\theta, \sqrt{N}x) \\ N^{-1/2} \nabla_x U(\theta, \sqrt{N}x) \end{pmatrix}.$$

Let us now introduce $z_\theta \in \mathbb{R}^{d_\theta}$ and $z_x = (z_1, \dots, z_N)^T$ where $z_i \in \mathbb{R}^{d_x}$ for $i = 1, \dots, N$. We define

$$\bar{U}_N(z_\theta, z_x) = \frac{1}{N} \sum_{i=1}^N U_N(z_\theta, z_i). \quad (16)$$

The gradients are given as

$$\nabla_{z_\theta} \bar{U}_N(z_\theta, z_x) = \frac{1}{N} \sum_{i=1}^N \nabla_\theta U(z_\theta, \sqrt{N} z_x^i), \quad \nabla_{z_x} \bar{U}_N(z_\theta, z_x) = \begin{pmatrix} N^{-1/2} \nabla_x U(z_\theta, \sqrt{N} z_1) \\ \vdots \\ N^{-1/2} \nabla_x U(z_\theta, \sqrt{N} z_N) \end{pmatrix}. \quad (17)$$

Next, let $\mathbf{Z}_t^i = N^{-1/2}\mathbf{X}_t^i$ for $i = 1, \dots, N$, $\mathbf{Z}_t = (\boldsymbol{\theta}_t, \mathbf{Z}_t^1, \dots, \mathbf{Z}_t^N)^\top \in \mathbb{R}^{d_\theta + Nd_x}$, $\bar{\mathbf{V}}_t^{z_i} = N^{-1/2}\mathbf{V}_t^{x_i}$ and $\bar{\mathbf{V}}_t^z = (\mathbf{V}_t^\theta, \bar{\mathbf{V}}_t^{z_1}, \dots, \bar{\mathbf{V}}_t^{z_N})^\top \in \mathbb{R}^{d_\theta + Nd_x}$. We can rewrite the system [KIPLD](#) as

$$\begin{aligned} d\mathbf{Z}_t &= \bar{\mathbf{V}}_t^z dt, \\ d\mathbf{V}_t^\theta &= -\gamma\mathbf{V}_t^\theta dt - \frac{1}{N} \sum_{i=1}^N \nabla_\theta U(\boldsymbol{\theta}_t, \sqrt{N}\mathbf{Z}_t^i) dt + \sqrt{\frac{2\gamma}{N}} d\mathbf{B}_t^0, \\ d\bar{\mathbf{V}}_t^{z_i} &= -\gamma\bar{\mathbf{V}}_t^{z_i} dt - N^{-1/2} \nabla_x U(\boldsymbol{\theta}_t, \sqrt{N}\mathbf{Z}_t^i) dt + \sqrt{\frac{2\gamma}{N}} d\mathbf{B}_t^i, \quad \text{for } i \in [N]. \end{aligned} \tag{18}$$

where \mathbf{B}_t^0 is a \mathbb{R}^{d_θ} -valued Brownian motion and \mathbf{B}_t^i for $i = 1, \dots, N$ are \mathbb{R}^{d_x} -valued Brownian motions. Rewriting the system (18) in terms of \bar{U}_N , using (17), we obtain the result. \square

We can also write the [KIPLD](#) in the following alternative way which will ease the analysis.

Lemma A.2 (KIPLD as a standard underdamped Langevin Diffusion). *The [KIPLD](#) diffusion can also be written as a single $d_\theta + Nd_x$ -dimensional underdamped Langevin diffusion given by*

$$\begin{aligned} d\tilde{\mathbf{Z}}_t &= \tilde{\mathbf{V}}_t^z dt, \\ d\tilde{\mathbf{V}}_t^z &= -\tilde{\gamma}\tilde{\mathbf{V}}_t^z dt - N\nabla_z \bar{U}_N(\tilde{\mathbf{Z}}_t) dt + \sqrt{2\tilde{\gamma}} d\mathbf{B}_t, \end{aligned} \tag{19}$$

where $\tilde{\mathbf{Z}}_t, \tilde{\mathbf{V}}_t^z \in \mathbb{R}^{d_x + Nd_\theta}$ are given as,

$$\tilde{\mathbf{Z}}_t = (\boldsymbol{\theta}_{\sqrt{N}t}, N^{-1/2}\mathbf{X}_{\sqrt{N}t}^1, \dots, N^{-1/2}\mathbf{X}_{\sqrt{N}t}^N)^\top, \quad \tilde{\mathbf{V}}_t^z = (\sqrt{N}\mathbf{V}_{\sqrt{N}t}^\theta, \mathbf{V}_{\sqrt{N}t}^{x_1}, \dots, \mathbf{V}_{\sqrt{N}t}^{x_N})^\top,$$

$(\mathbf{B}_t)_{t \geq 0}$ is a $\mathbb{R}^{d_\theta + Nd_x}$ -valued Brownian motion, $\tilde{\gamma} = \sqrt{N}\gamma$ and

$$\bar{U}_N(\boldsymbol{\theta}, z_1, \dots, z_N) := \frac{1}{N} \sum_{i=1}^N U(\boldsymbol{\theta}, z_i).$$

Proof. We use [25, Lemma 1] to prove this result. Consider the variables $\tilde{\mathbf{Z}}_t$ and $\tilde{\mathbf{V}}_t^z$. It is straightforward to observe that

$$d\tilde{\mathbf{Z}}_t = \tilde{\mathbf{V}}_t^z dt.$$

Indeed the space rescaling accounts for the time-rescaling in the dynamics of $\tilde{\mathbf{Z}}_t$. Now observe that

$$\begin{aligned} d\tilde{\mathbf{V}}_t^\theta &= -N\gamma\mathbf{V}_{\sqrt{N}t}^\theta dt - \nabla_\theta \sum_{i=1}^N U(\boldsymbol{\theta}_{\sqrt{N}t}, \mathbf{X}_{\sqrt{N}t}^i) dt + \sqrt{2\gamma\sqrt{N}} d\mathbf{B}_t^0 \\ &= -\sqrt{N}\gamma\tilde{\mathbf{V}}_t^\theta dt - N\nabla_\theta \bar{U}_N(\tilde{\mathbf{Z}}_t) dt + \sqrt{2\gamma\sqrt{N}} d\mathbf{B}_t^0. \end{aligned}$$

Similarly we obtain for $i \in [N]$,

$$\begin{aligned} d\tilde{\mathbf{V}}_t^{x_i} &= -\sqrt{N}\gamma\mathbf{V}_{\sqrt{N}t}^{x_i} dt - \nabla_x U(\boldsymbol{\theta}_{\sqrt{N}t}, \mathbf{X}_{\sqrt{N}t}^i) dt + \sqrt{2\gamma\sqrt{N}} d\mathbf{B}_t^i \\ &= -\sqrt{N}\gamma\tilde{\mathbf{V}}_t^{x_i} dt - \nabla_x \bar{U}_N(\tilde{\mathbf{Z}}_t) dt + \sqrt{2\gamma\sqrt{N}} d\mathbf{B}_t^i, \end{aligned}$$

where we recall our definition of the gradient of \bar{U}_N from (17) to obtain the correct scaling in front of $\nabla_x \bar{U}_N(\tilde{\mathbf{Z}}_t)$. Now, taking $\tilde{\gamma} = \sqrt{N}\gamma$, the result follows. \square

Recall that the algorithms proposed seek to target with the n th step the analytic solution at time $n\eta$, where η is the step-size of the algorithm for the rescaled system. Hence, by re-scaling $\tilde{\eta} = \frac{\eta}{\sqrt{N}}$, we can use algorithms for the rescaled system to produce estimates for [KIPLMC1](#) and [KIPLMC2](#). This is discussed below in [B.4](#) and [B.5](#). Given these results, it is natural to explore the properties of the function \bar{U}_N , as this new potential plays a crucial role in both rescalings. We note below some properties of \bar{U}_N which will be useful in the proofs.

Lemma A.3 (Stationary measure for (19)). *The measure $\tilde{\pi}$, left stationary by the dynamics of (19), is given as*

$$\tilde{\pi}(d\tilde{z}, d\tilde{v}) \propto \exp\left(-N\bar{U}_N(\tilde{z}) - \frac{1}{2}\|\tilde{v}\|^2\right) d\tilde{z}d\tilde{v}, \quad (20)$$

for all $\tilde{z}, \tilde{v} \in \mathbb{R}^{d_z}$.

This result follows directly by observing the rescaling given in Lemma A.2, both in the parameters and equation. For a discussion of the stationary measure of a standard underdamped Langevin diffusion see [55, Chapter 6].

Lemma A.4 (Strong convexity of \bar{U}_N). *Under H1, the function $\bar{U}_N : \mathbb{R}^{d_\theta + Nd_x} \rightarrow \mathbb{R}$ as defined in (16) is μ -strongly convex*

$$\langle z - z', \nabla \bar{U}_N(z) - \nabla \bar{U}_N(z') \rangle \geq \mu \|z - z'\|^2,$$

for all $z, z' \in \mathbb{R}^{d_\theta + Nd_x}$ and $N \in \mathbb{N}$.

Proof. Let $z = (z_\theta, z_1, \dots, z_N)$ and $z' = (z'_\theta, z'_1, \dots, z'_N)$. We have

$$\begin{aligned} \langle z - z', \nabla \bar{U}_N(z) - \nabla \bar{U}_N(z') \rangle &= \left\langle \begin{pmatrix} z_\theta - z'_\theta \\ z_1 - z'_1 \\ \vdots \\ z_N - z'_N \end{pmatrix}, \begin{pmatrix} (1/N) \sum_{i=1}^N (\nabla_\theta U(z_\theta, \sqrt{N}z_i) - \nabla_\theta U(z'_\theta, \sqrt{N}z'_i)) \\ N^{-1/2} \nabla_x U(z_\theta, \sqrt{N}z_1) - N^{-1/2} \nabla_x U(z'_\theta, \sqrt{N}z'_1) \\ \vdots \\ N^{-1/2} \nabla_x U(z_\theta, \sqrt{N}z_N) - N^{-1/2} \nabla_x U(z'_\theta, \sqrt{N}z'_N) \end{pmatrix} \right\rangle \\ &= \frac{1}{N} \sum_{i=1}^N \left(\langle z_\theta - z'_\theta, \nabla_\theta U(z_\theta, \sqrt{N}z_i) - \nabla_\theta U(z'_\theta, \sqrt{N}z'_i) \rangle \right) \\ &\quad + \frac{1}{N} \sum_{i=1}^N \langle N^{1/2}z_i - N^{1/2}z'_i, \nabla_x U(z_\theta, \sqrt{N}z_i) - \nabla_x U(z'_\theta, \sqrt{N}z'_i) \rangle. \end{aligned}$$

Next, H1 implies that

$$\langle z - z', \nabla \bar{U}_N(z) - \nabla \bar{U}_N(z') \rangle \geq \frac{1}{N} \sum_{i=1}^N \mu (\|z_\theta - z'_\theta\|^2 + N\|z_i - z'_i\|^2) = \mu \|z - z'\|^2.$$

This completes the proof. \square

Next, we show that the function \bar{U}_N is L -gradient Lipschitz.

Lemma A.5 (Gradient Lipschitzness of \bar{U}_N). *Under H2, the function $\bar{U}_N : \mathbb{R}^{d_\theta + Nd_x} \rightarrow \mathbb{R}$ as defined in (16) is L -gradient Lipschitz*

$$\|\nabla \bar{U}_N(z) - \nabla \bar{U}_N(z')\| \leq L \|z - z'\|,$$

for all $z, z' \in \mathbb{R}^{d_\theta + Nd_x}$ and $N \in \mathbb{N}$.

Proof. Let $z = (z_\theta, z_1, \dots, z_N)$ and $z' = (z'_\theta, z'_1, \dots, z'_N)$. Then

$$\begin{aligned} \|\nabla \bar{U}_N(z) - \nabla \bar{U}_N(z')\|^2 &= \left\| \begin{pmatrix} (1/N) \sum_{i=1}^N \nabla_\theta U(z_\theta, \sqrt{N}z_i) - \nabla_\theta U(z'_\theta, \sqrt{N}z'_i) \\ N^{-1/2} \nabla_x U(z_\theta, \sqrt{N}z_1) - N^{-1/2} \nabla_x U(z'_\theta, \sqrt{N}z'_1) \\ \vdots \\ N^{-1/2} \nabla_x U(z_\theta, \sqrt{N}z_N) - N^{-1/2} \nabla_x U(z'_\theta, \sqrt{N}z'_N) \end{pmatrix} \right\|^2 \\ &= \left\| \frac{1}{N} \sum_{i=1}^N \left(\nabla_\theta U(z_\theta, \sqrt{N}z_i) - \nabla_\theta U(z'_\theta, \sqrt{N}z'_i) \right) \right\|^2 \\ &\quad + \frac{1}{N} \sum_{i=1}^N \left\| \nabla_x U(z_\theta, \sqrt{N}z_i) - \nabla_x U(z'_\theta, \sqrt{N}z'_i) \right\|^2. \end{aligned}$$

Using the fact that $(\cdot)^2$ is a convex function and Jensen's inequality for the first term, we obtain

$$\begin{aligned} \|\nabla \bar{U}_N(z) - \nabla \bar{U}_N(z')\|^2 &\leq \frac{1}{N} \sum_{i=1}^N \left\| \nabla_\theta U(z_\theta, \sqrt{N}z_i) - \nabla_\theta U(z'_\theta, \sqrt{N}z'_i) \right\|^2 \\ &\quad + \frac{1}{N} \sum_{i=1}^N \left\| \nabla_x U(z_\theta, \sqrt{N}z_i) - \nabla_x U(z'_\theta, \sqrt{N}z'_i) \right\|^2. \end{aligned}$$

Using [H2](#), we have

$$\begin{aligned} \|\nabla \bar{U}_N(z) - \nabla \bar{U}_N(z')\|^2 &\leq \frac{L^2}{N} \sum_{i=1}^N (\|z_\theta - z'_\theta\|^2 + N\|z_i - z'_i\|^2) \\ &= L^2 \|z - z'\|^2, \end{aligned}$$

which completes the proof. \square

B Proofs

B.1 Proof of Proposition 1

Given Lemma [A.1](#), the system [\(15\)](#) has a positive recurrent Markov stationary measure, absolutely continuous with respect to the Lebesgue measure, given by the density [\[34\]](#)

$$\bar{\pi}^N(z, \bar{v}) \propto \exp \left(-N\bar{U}_N(z) - \frac{N}{2} \|\bar{v}\|^2 \right),$$

where \bar{U}_N is given in [\(16\)](#). Note, this follows from eqs. (1.1) and (1.3) in [\[34\]](#) by putting $U := N\bar{U}_N$ and $u = N^{-1}$. Let $z = (\theta, z_1, \dots, z_N)$. Using [\(16\)](#), we have

$$\bar{\pi}(z, \bar{v}) \propto \exp \left(- \sum_{i=1}^N U(\theta, \sqrt{N}z_i) - \frac{N}{2} \|\bar{v}\|^2 \right).$$

Let us now look at θ -marginal of this density, which can be written as

$$\pi_\Theta^N(\theta) \propto \int_{\mathbb{R}^{Nd_x + d_\theta}} \int_{\mathbb{R}^{Nd_x}} e^{-\sum_{i=1}^N U(\theta, \sqrt{N}z_i) - \frac{N}{2} \|\bar{v}\|^2} dz_x d\bar{v}.$$

where $z_x = (z_1, \dots, z_N) \in \mathbb{R}^{Nd_x}$. Note now that, integrating out \bar{v} , using a change of variables $x'_i = \sqrt{N}z_i$, and setting $x' = (x'_1, \dots, x'_N)$, we have

$$\begin{aligned} \pi_{\Theta}^N(\theta) &\propto N^{-1/2} \int_{\mathbb{R}^{Nd_x}} e^{-\sum_{i=1}^N U(\theta, x'_i)} dx', \\ &\propto \left(\int_{\mathbb{R}^{d_x}} e^{-U(\theta, x')} dx' \right)^N = \exp(N \log p_{\theta}(y)), \end{aligned}$$

since $p_{\theta}(y) = \int e^{-U(\theta, x)} dx$ by definition where $U(\theta, x) = -\log p_{\theta}(x, y)$.

B.2 Proof of Proposition 2

Note that, by [H1](#), $U(\theta, x)$ is jointly μ -strongly convex. Let $\kappa(\theta) = -\log p_{\theta}(y)$. Using the Prekopa-Leindler inequality for strongly log-concave distributions [[62](#), Theorem 3.8], we can see that

$$\langle \theta - \theta', \nabla \kappa(\theta) - \nabla \kappa(\theta') \rangle \geq \mu \|\theta - \theta'\|^2.$$

The bound then follows using an identical proof of Proposition 3 in [[3](#)].

B.3 Proof of Proposition 3

The proof follows from Lemma [A.1](#) which shows that we can rewrite the [KIPLD](#) system as a single $d_{\theta} + Nd_x$ -dimensional underdamped Langevin diffusion. Then with a suitable time rescaling (see Lemma 1 in [[25](#)]), we can rewrite this diffusion as a standard underdamped diffusion as shown in Lemma [A.2](#). The result then follows from the exponential convergence of the underdamped Langevin diffusion [[25](#), Theorem 1] with suitable modifications, e.g., see the proof of [[44](#), Theorem 8.7]. The result then follows from the fact that W_2 between marginals are bounded by the W_2 between joint distributions.

B.4 Proof of Theorem 1

By Lemma [A.2](#), we have the standard underdamped diffusion

$$\begin{aligned} d\tilde{\mathbf{Z}}_t &= \tilde{\mathbf{V}}_t^z dt, \\ d\tilde{\mathbf{V}}_t^z &= -\tilde{\gamma} \tilde{\mathbf{V}}_t^z dt - N \nabla_z \bar{U}_N(\tilde{\mathbf{Z}}_t) dt + \sqrt{2\tilde{\gamma}} d\mathbf{B}_t. \end{aligned} \tag{21}$$

It is apparent that the stationary measure of this scheme is

$$\tilde{\pi}(z, v) \propto e^{-N\bar{U}_N(z) - \frac{1}{2}\|v\|^2}.$$

We will now look at the standard kinetic Langevin Monte Carlo discretisation of the SDE in (21) and show that this scheme coincides with [KIPLMC1](#). Thus we can utilize the bounds in [[25](#)] directly for our scheme.

Let us write the Exponential Integrator discretisation of this scheme (abusing the notation using same letters) using the step-size $\tilde{\eta}$

$$\begin{aligned} \tilde{\mathbf{Z}}_{n+1} &= \tilde{\mathbf{Z}}_n + \tilde{\psi}_1(\tilde{\eta}) \tilde{\mathbf{V}}_n^z - \tilde{\psi}_2(\tilde{\eta}) N \nabla \bar{U}_N(\tilde{\mathbf{Z}}_n) + \sqrt{2\tilde{\gamma}} \tilde{\varepsilon}_{n+1}, \\ \tilde{\mathbf{V}}_{n+1}^z &= \tilde{\psi}_0(\tilde{\eta}) \tilde{\mathbf{V}}_n^z - \tilde{\psi}_1(\tilde{\eta}) N \nabla \bar{U}_N(\tilde{\mathbf{Z}}_n) + \sqrt{2\tilde{\gamma}} \tilde{\varepsilon}'_{n+1}. \end{aligned} \tag{22}$$

Since the function $z \mapsto N\bar{U}_N(z)$ is $N\mu$ strongly convex and NL -gradient-Lipschitz, for $\tilde{\gamma} \geq \sqrt{N\mu + NL}$ and $\tilde{\eta} \leq m/(4\tilde{\gamma}L)$, [[25](#), Theorem 2] directly implies that

$$W_2(\nu_n, \tilde{\pi}) \leq \sqrt{2} \left(1 - \frac{0.75\mu\tilde{\eta}}{\tilde{\gamma}} \right)^n W_2(\nu_0, \tilde{\pi}) + \frac{L\tilde{\eta}\sqrt{2d_z}}{\mu},$$

where ν_n denotes the law of the discretisation (22) at time n and $\tilde{\pi}$ the stationary measure given in Lemma A.3. We relate the discretisation (22) to KIPLMC1. It is straightforward to check that, after proper modifications, the discretisation (22) coincides with the KIPLMC1 with $\tilde{\eta} = \eta/\sqrt{N}$ and $\tilde{\gamma} = \sqrt{N}\gamma$. Therefore, by specializing this bound to θ -dimension and substituting $\tilde{\eta} = \eta/\sqrt{N}$ and $\tilde{\gamma} = \sqrt{N}\gamma$, we obtain the convergence bound for the KIPLMC1. Combining this with the concentration result from Prop. 2, we obtain the result.

B.5 Proof of Theorem 2

Again, recall by Lemma A.2, we consider our rescaled standard underdamped diffusion, given by (21) and seek to recover from this the behaviour of KIPLMC2. Using this rescaled system we directly apply the results from [53] for our scheme.

We now write the splitting scheme for the diffusion in Lemma A.2, using step-size $\tilde{\eta}$,

$$\begin{aligned}\tilde{\mathbf{Z}}_{n+1} &= \tilde{\mathbf{Z}}_n + \tilde{\eta}(\tilde{\delta}\tilde{\mathbf{V}}_n^z + \sqrt{1 - \tilde{\delta}^2}\varepsilon_{n+1}) - \frac{\tilde{\eta}^2}{2}N\nabla\bar{U}_N(\tilde{\mathbf{Z}}_n) \\ \tilde{\mathbf{V}}_{n+1}^z &= \tilde{\delta}^2\tilde{\mathbf{V}}_n^z - \frac{\tilde{\eta}\tilde{\delta}}{2}(N\nabla\bar{U}_N(\tilde{\mathbf{Z}}_n) + N\nabla\bar{U}_N(\tilde{\mathbf{Z}}_{n+1})) + \sqrt{1 - \tilde{\delta}^2}(\tilde{\delta}\varepsilon_{n+1} + \varepsilon'_{n+1}),\end{aligned}\tag{23}$$

where $\tilde{\delta} = e^{-\tilde{\gamma}\tilde{\eta}/2}$. Using the NL -gradient-Lipschitzness and $N\mu$ strong convexity of the function $z \mapsto N\bar{U}_N(z)$, and with the choice of $\tilde{\gamma} \geq 2\sqrt{NL}$ and $\tilde{\eta} \leq \frac{N\mu}{33\tilde{\gamma}^3}$, we apply the results of [53, Theorem 1] and [53, Proposition 11] to obtain

$$W_2(\nu_n, \tilde{\pi}) \leq \tilde{C} \left(\left(1 - \frac{\tilde{\eta}\tilde{\mu}}{\tilde{\gamma}}\right)^{\frac{n}{2}} W_2(\nu_0, \tilde{\pi}) + \tilde{\eta}\sqrt{2d_z}\frac{6\tilde{\gamma}\tilde{K}}{\tilde{\mu}} \right),$$

where ν_n is now the law of the discretisation (23) at time n and $\tilde{\pi}$ the stationary measure from Lemma A.3. Further,

$$\tilde{C} = \sqrt{3}(\sqrt{NL} \vee \sqrt{NL}^{-1}), \quad \tilde{K} = NL \left(1 + e^{NL\tilde{\eta}^2} \left(\frac{\tilde{\eta}}{6} + \frac{\tilde{\eta}^2 NL}{24} \right) \right) \left(1 + \frac{\tilde{\eta}NL}{2\sqrt{\tilde{\mu}}} \right).$$

Again, we can recover the behaviour of KIPLMC2 when we set $\tilde{\eta} = \eta/\sqrt{N}$ and $\tilde{\gamma} = \sqrt{N}\gamma$. It is quite easy to see that when we set these parameters and consider the θ -marginal, the n th step of this rescaled scheme will now correspond to the n th step of the KIPLMC2, provided the initial distribution of both is the same. Combining this with the concentration result from Prop. 2, we obtain the desired result.

C Results

C.1 Area Between Curve Calculation (ABC)

To compare the behaviour of the different algorithms, we seek to identify a measure that quantifies how accurately and quickly each algorithm converges to the true solution. To do this we employ the ABC to do this, as in [49]. Consider $c^k : \mathbb{N} \rightarrow \mathbb{R}$ and $c^m : \mathbb{N} \rightarrow \mathbb{R}$ to be the accuracy curves of KIPLMC2 and MPGDnc respectively, i.e. for $\{\theta_n\}_{n=1}^\infty$ generated by the KIPLMC2 algorithm, $c^k(n) = \|\theta_n - \bar{\theta}^*\|$. The ABC we will compute is,

$$\sum_{i=1}^M w(i)(c^m(i) - c^k(i)),$$

where M is the total number of time-steps and w acts as a normalising, weighting function. We set $w(i) = \frac{2}{M(M+1)}\frac{i}{M}$ for our computations, as it matches the weighting used in [47]. Hence, the ABC computes a signed, weighted area between the error curves of MPGD and KIPLMC2. In particular, when c^m is dominated by c^k , the ABC is negative, whilst positive in the converse case.

C.2 Variance from (c) Fig. 3 in tabular form

Table 2: We compare the performance of the different algorithms over increasing step-sizes. Observe, despite the better behaviour at lower step-size η , the MPGDnc algorithm is the least stable. We compute the sample variance of the algorithms over 20 Monte Carlo simulations, using the last 500 steps of each simulation.

Algorithms	Sample Variance				
	0.01	0.025	η 0.05	0.075	0.1
MPGDnc	2.30×10^{-2}	2.77×10^{-2}	1.75×10^9	2.34×10^{50}	7.78×10^{110}
KIPLMC1	1.91×10^{-1}	1.30×10^{-1}	1.90×10^{-1}	8.52×10^{-1}	6.06×10^{17}
KIPLMC2	2.63×10^{-2}	3.05×10^{-2}	3.37×10^{-2}	3.03×10^{-2}	3.36×10^{-2}

C.3 Error Metrics for the BNN

Recall that the output of our model for latent variable $x = (w, v)$, image features f is,

$$p(l|f, x) \propto \exp \left(\sum_{j=1}^{40} v_{lj} \tanh \left(\sum_{i=1}^{784} w_{ji} f_i \right) \right).$$

To normalise the outputs of the RHS over the labels we apply softmax to the estimates for all l . Denote this as $g(l|f, x)$ and we give the output of the model as

$$\hat{l}(f|x) = \operatorname{argmax}_{l \in \{0,1\}} g(l|f, x).$$

For the BNN in 5.3 we use two metrics to evaluate the performance of our models, which we evaluate on test set of 200 images and labels $\mathcal{Y}_{\text{test}}$. In particular we use a relative error metric, measuring the percentage accuracy on the test set,

$$\frac{1}{|\mathcal{Y}_{\text{test}}|} \sum_{(f,l) \in \mathcal{Y}_{\text{test}}} |l - \hat{l}(f|x)|.$$

A second measure, which in our case is more discriminating, is the log pointwise predictive density (LPPD). This returns the average log probability assigned by the model to the correct label, given as,

$$\frac{1}{|\mathcal{Y}_{\text{test}}|} \sum_{(f,l) \in \mathcal{Y}_{\text{test}}} \log g(l|f, x).$$

Indeed, by [47], assuming that the data generating process produces independent samples, then this metric approximates the difference of the Kullback-Leibler divergence and the entropy of the data generating process. Indeed, the LPPD approximates

$$\begin{aligned} \int \log g(l|f, x) p(dl, df) &= \int \int \log \left(\frac{g(l|f)}{p(l|f)} \right) p(dl|df) p(df) + \int \log p(l|f) p(dl, df) \\ &= - \int \text{KL}(g(\cdot|f) \| p(\cdot|f)) p(df) + \int \log p(l|f) p(dl, df), \end{aligned}$$

where $p(l, f)$ is density from which the data is independently sampled. Hence, the larger the LPPD, the smaller the Kullback-Leibler divergence between our estimate and the true distribution.